UNIVERSITA' DEGLI STUDI
DI PADOVA

DIPARTIMENTO DI SCIENZE DEL
FARMACO

DIPARTIMENTO DI SCIENZE
BIOMEDICHE

**CORSO DI LAUREA MAGISTRALE IN
PHARMACEUTICAL BIOTECHNOLOGIES –
BIOTECNOLOGIE FARMACEUTICHE**

TESI DI LAUREA

Characterization of wild-type and folding-defective mutants of galactosylceramidase

Caratterizzazione della forma wild-type e di mutanti folding-defective della proteina galattosilceramidasi

RELATORE: DR. ESSA DORIANNA SANDONÀ
CONTRORELATORE: DR. ESSA LAURA ACQUASALIENTE
SUPERVISOR: DR. MAURIZIO MOLINARI

LAUREANDO: FABBRO MARCO

ANNO ACCADEMICO 2021/2022

ABSTRACT

In the process of protein synthesis, almost 40% of the total polypeptide chains are translocated into the endoplasmic reticulum (ER), where they begin their maturation process. The ER has a very refined and complex system of quality control, ensuring that only properly folded proteins can continue their journey through the Golgi apparatus, from where they are sent to their final destinations. Meanwhile, misfolded proteins that fail to acquire their native structure are retained into the ER, where they are sent to degradation through ER-associated degradation (ERAD) or ER-to-lysosome-associated degradation (ERLAD).

Galactosylceramidase (GALC) is a lysosomal hydrolase responsible for sphingolipids metabolism, essential for the maintenance of the myelin sheath along nerves. Mutations along the coding sequence of this protein are responsible for folding-defective variants, which accumulate inside the ER causing toxicity and cell death in the central nervous system (CNS). The inability of GALC to effectively participate in the sphingolipids metabolism leads to a lysosomal storage disorder (LSD) called Krabbe disease. Patients affected by this disease present severe damage at the level of their CNS, caused by cell death for toxic accumulation of metabolic intermediates and for the absence of myelin along the nervous system.

In this work we study the wild-type form of GALC and four of its mutants, trying to find a proper readout to assess if the enzyme is being correctly folded or not. Our results show that properly folded GALC completes its maturation process and it is secreted outside the cell, while folding-incompetent variants are not secreted, as they are retained inside the ER.

RIASSUNTO

Nel processo di sintesi proteica, quasi il 40% dei polipeptidi totali viene traslocato nel reticolo endoplasmatico (RE), dove inizia il processo di maturazione. Il RE dispone di un sistema di controllo della qualità molto raffinato e complesso, garantendo che solo le proteine correttamente ripiegate possano continuare il loro viaggio attraverso l'apparato di Golgi, da dove vengono inviate alle loro destinazioni finali. Le proteine mal ripiegate che non riescono ad acquisire la loro struttura nativa vengono trattenute nell'ER, dove vengono avviate alla degradazione attraverso la degradazione associata al RE (ERAD) o la degradazione associata dal RE al lisosoma (ERLAD).

La galattosilceramidasi (GALC) è un'idrolasi lisosomiale responsabile del metabolismo degli sfingolipidi, essenziale per il mantenimento della guaina mielinica lungo i nervi. Le mutazioni lungo la sequenza codificante di questa proteina sono responsabili di varianti che non riescono a ripiegarsi correttamente, accumulandosi all'interno dell'ER e causando tossicità e morte cellulare nel sistema nervoso centrale (SNC). L'incapacità di GALC di partecipare efficacemente al metabolismo degli sfingolipidi porta ad una malattia da accumulo lisosomiale (LSD) chiamata malattia di Krabbe. I pazienti affetti da questa malattia presentano gravi danni a livello del SNC, causati dalla morte cellulare per tossicità da accumulo di intermedi metabolici e per l'assenza di mielina lungo il sistema nervoso.

In questo lavoro di tesi studiamo la forma wild type di GALC e quattro suoi mutanti (G41S, G270D, T513M, Y551S), cercando di trovare una procedura adeguata a valutare se l'enzima è ripiegato correttamente o meno. Questi studi potranno essere usati come modello per testare eventuali farmaci, disegnati per aiutare i mutanti di GALC ad acquisire una corretta struttura proteica.

Sono stati generati cinque plasmidi, uno per ogni variante analizzata, con lo scopo di transfettare cellule di mammifero e permetterci di studiare il

processo di maturazione di GALC. Abbiamo dimostrato che le varianti di GALC che riescono a piegarsi correttamente vengono secrete nel terreno di coltura, mentre le varianti che non si ripiegano correttamente vengono ritenute all'interno della cellula.

Abbreviations

ATZ	Alpha1-antitrypsin Z
BBB	Blood brain barrier
BiP	Binding immunoglobulin protein
CD-MPR	Cation dependent mannose-6-phosphate receptor
CI-MPR	Cation independent mannose-6-phosphate receptor
CNS	Central nervous system
CNX	Calnexin
COPII	Cytosolic coatomer protein II
CRT	Calreticulin
ER	Endoplasmic reticulum
ERAD	ER-associated degradation
ERLAD	ER-to-lysosome-associated degradation
ERT	Enzyme replacement therapies
GALC	Galactosylceramidase
KD	Krabbe disease
LC3II	Microtubule associated protein 1 light chain 3 II
LSD	Lysosomal storage disorder
M6P	Mannose-6-phosphate
NBD	Nucleotide binding domain
OS-9	Osteosarcoma amplified-9 protein
OST	Oligosaccharyl-transferase complex
PDI	Protein disulphide isomerase

SBD	Substrate binding domain
SRP	Signal recognition particle
TRAM	Translocating chain-association membrane protein
TRAP	Translocon-associated protein
UGGT1	UDP-glucose:glycoprotein glucosyltransferase
UPR	Unfolded protein response
XTP3-B	XTP3-transactivated gene-B

TABLE OF CONTENTS

1. INTRODUCTION

1.1. The endoplasmic reticulum (ER)

1.1.1. ER structure and main functions

The endoplasmic reticulum is one of the most important organelles within the cell, where approximately 40% of the total cellular proteome is produced (Braakman and Bulleid 2011). This organelle is organized in a reticular membranous structure directly connected to the nuclear membrane and it can be divided in two different parts, rough and smooth. Rough ER has ribosomes on the cytosolic surfaces and it is responsible for the synthesis and post-translational modifications for secreted and membrane bound proteins. On the other hand, smooth ER plays an important role in detoxification and lipid synthesis. Proteins that enter the ER need to fold correctly to pass the quality-control checkpoints of the cell, before being transported to the Golgi network for further modifications (Schwarz and Blower 2016).

1.1.2. Protein synthesis and translocation inside the ER

When the polypeptide chain starts to emerge from the cytosolic ribosomes, a signal sequence of hydrophobic amino acids (Kriegler et al. 2018) on the N-terminal is recognized by a ribonucleoprotein called signal recognition particle (SRP). The complex made by the polypeptide and the SRP then binds to the ER membrane through the SRP receptor and the polypeptide chain can be translocated inside the ER with the help of the translocation machinery and hydrolysis of GTP (Braakman and Bulleid 2011).

Sec61 is the main channel in eukaryote organisms, which is a complex of transmembrane proteins made by three subunits, Secα, Secβ and Secγ, the signal peptidase complex, responsible for the cleavage of the signal peptides, the translocating chain-association membrane protein (TRAM),

the oligosaccharyl-transferase complex (OST) and the translocon-associated protein (TRAP) (Pfeffer et al. 2016). This complex forms a channel in the ER membrane, through which the polypeptide chain can enter the ER lumen. This strategy of co-translational translocation is very useful, because it precludes premature protein folding and it exploits part of the energy of the translational process for the translocation (Cross, Sinning et al. 2009).

1.1.3. N-glycosylation in the ER

An important function of the ER is the glycosylation of newly synthesised proteins through the addition of a common sugar chain on asparagine (N) residues. Sugar chains are not added on all N residues, because they need a consensus sequence along the polypeptide chain consisting in N-X-S/T, where N is the asparagine residue where the sugar is attached, X is any amino acid except proline, S/T are serine or threonine (Aebi 2013). The sugar chain is made by a total of 14 sugars, which include 3 glucose residues, 9 mannose residues and 2 N-acetylglucosamine residues ($Glc_3Man_9GlcNAc_2$), which are linked in this order starting from the N-acetylglucosamine attached to the N residue of the protein (Fregno, Fasana et al. 2021). These glycans are then trimmed by glucosidase I and II, causing the removal of two glucose residues. The resulting protein will be ready for the binding of ER chaperones, such as calnexin (CNX) and calreticulin (CRT), essential for the folding process and acquisition of the native structure (Kozlov and Gehring 2020).

1.1.4. Protein folding in the ER

Protein folding in the ER is aided by enzymes, such as the protein disulphide isomerase (PDI) and molecular chaperones, such as BiP, CNX and CRT. These proteins are essential to prevent aggregation of newly synthesised polypeptides and to assist them during the folding process (Hebert and Molinari 2007).

PDI catalyses the oxidation of free SH groups on cysteines to form disulphide bonds and help proteins to acquire their correct tertiary structure (Braakman and Bulleid 2011). BiP belongs to the family of Hsp70 proteins and is a major component of the translocation machinery for protein import in the ER. It has two main structural domains, a nucleotide binding domain (NBD) and a substrate binding domain (SBD). Other than helping in the folding process of proteins, this molecular chaperone has other important functions, such as regulator for Ca2+ homeostasis, facilitator of ERAD and it is also involved in the unfolded protein response (UPR) (Wang et al. 2017). Calnexin and calreticulin are two carbohydrate binding proteins, also called lectins, which need Ca^{2+} for their activity. They bind to mono-glycosylated proteins and help to retain them into the ER to achieve a correct folding state (Brodsky and Skach 2011). CNX has two main structural components: a lectin-like glycan-binding domain with a flexible arm and the P-domain that has the purpose of recruiting other chaperones (Kozlov and Gehring 2020). CRT is the soluble homolog of CNX, where the first one preferentially binds protein close to the ER membrane, while the second one preferentially binds peripheral proteins (Lamriben et al. 2016). When proteins are released from the binding with CNX or CRT, the last glucose is removed by glucosidase II, preventing another binding with lectin chaperones. In the case the polypeptide still fails to fold correctly, a glucose is newly added by UDP-glucose-glycoprotein glucosyltransferase (UGGT1), making the protein suitable for a new binding with CNX or CRT (Kuribara et al. 2021).

1.1.5. ERAD

When proteins cannot properly acquire their native structures, they need to be cleared from the ER, otherwise they could undergo aggregation and accumulation, with severe consequences for cellular health. Degradation processes occurring to ER-resident misfolded proteins can be divided in ER-associated degradation (ERAD) or ER-to-lysosome-associated degradation

(ERLAD) (Fregno, Fasana et al. 2021). ERAD is a term indicating all pathways that lead to the export of misfolded proteins into the cytosol for proteasomal degradation. When misfolded proteins spend excessive time inside the ER, their oligosaccharides start to be trimmed by ER-resident α1,2-mannosidases (leaving 5-7 mannose residues). This indicates that the polypeptide is persistently unable to acquire its native structure and it must be sent for degradation (Fregno and Molinari 2019). After de-mannosylation misfolded proteins are recognized by osteosarcoma amplified-9 protein (OS-9) and XTP3-transactivated gene-B (XTP3-B), which are part of complexes named “dislocons” or “retrotranslocons”, that transport the protein outside the ER membrane for 26S proteasomes degradation (Hebert and Molinari 2012) (Fregno and Molinari 2019).

1.1.6. ERLAD

There are some cases where misfolded proteins are not suitable for ERAD degradation, such as when they undergo aggregation, forming polymers and impairing dislocation, or when they fail to engage with the ERAD quality control machinery (Fregno et al. 2018). To achieve clearance of ERAD-resistant polypeptides, they are delivered to endo-lysosomal compartments for degradation. This is mediated by autophagic or non-autophagic pathways, collectively known as ERLAD (Fregno and Molinari 2019).

A key example on how ERLAD works is found in the degradation of ERAD-resistant alpha1-antitrypsin Z (ATZ) (Fregno et al. 2018). ATZ polymers, too large to be translocated outside the ER membrane, are segregated in specific ER compartments with the assistance of CNX. In these subdomains, they interact with FAM134B, an important ER-membrane protein involved also in ER autophagy processes (Reggiori and Molinari 2022), which subsequently associates with microtubule associated protein 1 light chain 3 II (LC3II). This interaction promotes the docking of ER-derived vesicles to RAB7/LAMP1-positive endolysosomes. Finally, with the involvement of SNARE STX17 and

SNARE VAMP8, the polymers are released inside endolysosomes for degradation (Fregno et al. 2018).

1.1.7. ER autophagy (ER-phagy)

Another important process occurring in the cell is the turnover of ER portions, which are sent for degradation to lysosomes or vacuoles. This process is called ER-phagy and it is fundamental for cellular functioning. It takes place for a wide variety of reasons, such as mobilizing metabolites after nutrient shortage, control ER size and activity, reestablishment of ER homeostasis after ER stresses and removal of ER subdomains where cytotoxic material is segregated. These processes are driven by specific ER-phagy receptors that, after activation, interact with members of the autophagy-related gene 8 (Atg8)/LC3 protein family, plus a wide variety of luminal and cytosolic proteins (Reggiori and Molinari 2022).

In this work three ER-phagy receptors will be analysed: SEC62, FAM134B and TEX264. SEC62 is an integral ER membrane protein, with two trans-membrane segments. It is a member of the translocon complex, being responsible for the translocation of newly synthesised proteins in the ER. It is a critical molecular component in maintenance of cellular and ER homeostasis (Fumagalli et al. 2016). FAM134B is an intra-membrane ER-resident protein that has a reticulon homology domain (RHD) and a LC3-interacting region (LIR) sequence (Reggio et al. 2021). It has a role on basal ER-phagy and it has been found to promote lysosomal clearance of ER subdomains containing misfolded proteins (Fregno et al. 2018). TEX264 is a single type-I trans-membrane ER protein of 313 amino acids (Reggiori and Molinari 2022) and it has been identified as an ER-phagy receptor in response of several stimuli, such as nutrient starvation (Chino et al. 2019).

1.2. Intracellular protein trafficking

1.2.1. Transport from the ER to the Golgi network

When the folding process is completed and the protein is suitable for further processing, it is transported from the ER to the Golgi network through membrane-enclosed containers, called transport vesicles. These containers are formed from the donor compartment and they deliver their cargo in the receiving compartment.

Proteins leaving the ER are transported in COPII-coated transport vesicles and exit the ER from special regions where ribosomes are not present on the membrane, called ER exit sites. COPII is a coat complex, made by several proteins and consisting in two layers. The inner layer is made by Sar1-Sec23-Sec24, while the outer is made by Sec13-Sec31 heterotetramers (Peotter, Kasberg et al. 2019). The vesicle coat has a double function. On the outside, the proteins responsible for the coating give a shape to the vesicle, bending the membrane and engulfing the proteins. On the inside of the vesicle, specific factors select which are the appropriate polypeptides for the transport and perform a selection to avoid the transport of undesired proteins.

After their formation, coated vesicles start to fuse with each other, through the SNAREs proteins. These specialized proteins allow membrane fusion interacting with each other. They are present on membranes in two types, v-SNAREs and t-SNAREs (Martens and McMahon 2008). Lastly, these clusters of vesicles move along microtubules and fuse with the Golgi network membrane, where their cargo is delivered and subjected to further modifications.

1.2.2. Oligosaccharide chains processing

In the Golgi apparatus, sugars attached to N-glycosylated proteins are subjected to further modifications by membrane bound glycosidases and

glycosyl transferases and they can be converted in complex oligosaccharides or high mannose oligosaccharides, which are the two main classes of oligosaccharides attached to mammalian proteins (Stanley 2011).

High mannose oligosaccharides usually contain eight or nine mannose residues and in some cases they remain unchanged during their passage through the Golgi and are exposed on proteins when they are secreted or inserted into the membrane (Stanley, Schachter et al. 2009). In the majority of cases glycans are processed by α-mannosidases and glycosyltransferases, removing mannose residues and adding galactose, sialic acid or other sugars, branching the structure up to six times, turning these sugar chains in complex oligosaccharides (Stanley 2011).

Regarding O-glycosylated proteins, in the Golgi apparatus they are extended by adding galactose, sialic acid, N-acetylgalactoseamine (GalNAc) or fucose, resulting in linear or branched sugar chains (Brockhausen, Schachter et al. 2009).

1.2.3. Transport from the Golgi network to lysosomes

After protein have passed through the Golgi apparatus, they can take different paths depending on their function and final localization. An important destination of intracellular trafficking are lysosomes. These organelles are responsible for the degradation of a broad range of biological macromolecules, like proteins, lipids, nucleic acids or carbohydrates (Hesketh, Wartosch et al. 2018) and they also take part in important cellular processes: they have the ability to sense nutrient levels within the cell, trigger proinflammatory responses and they have a critical role in lipid homeostasis and lipid mediated signalling (Ballabio and Bonifacino 2020).

Macromolecules can be delivered to lysosomes through different pathways. They can be taken by the extracellular environment through endocytosis or phagocytosis, depending on the dimensions of what is being engulfed. During endocytosis the cells internalize macromolecules, while during

phagocytosis cells internalize microorganisms or large particles, being the case of the immune system cells. Another important delivery route is autophagy, consisting in selective capture of macromolecules, portions of organelles and pathogens by degradative compartments of the cell. This process can be nonselective (or bulk) when the delivered cargo has an heterogenous composition, while it can be selective if the delivered cargo is specific and homogenous (Reggiori and Molinari 2022).

Looking in depth at the route from the Golgi network to lysosomes, necessary for the delivery of lysosomal enzymes, a mannose-6-phosphate (M6P) based-system is involved. Lysosomal hydrolases are marked with M6P on N-glycosylated residues and they are recognized by specific receptors in the Golgi, allowing their delivery to endosomes and lysosomes (Braulke and Bonifacino 2009).

When lysosomal enzymes arrive in the Golgi, they are recognized by a phosphotransferase, that transfers a N-acetylglucoseamine (GlcNAc) – 1 – phosphate residue to C6 positions of selected mannoses in high mannose type oligosaccharides of the selected protein. Then the terminal GlcNAc residue is removed by another enzyme, known as uncovering enzyme, exposing the M6P recognition signal. This signal is recognized by receptors in the Golgi which, after the binding with the marked protein, are packed inside vesicles and delivered to endosomes and lysosomes (Coutinho, Prata et al. 2012). The main receptors responsible for the recognition of M6P signals are dimeric type I membrane proteins, divided in the 46 kDa cation-dependent mannose 6-phosphate receptor (CD-MPR) and the 300 kDa cation-independent mannose 6-phosphate receptor (CI-MPR) (Castonguay, Olson et al. 2011). Once inside lysosomes, the acidic pH causes a dissociation of the protein from the M6P receptor, that can be retrieved and delivered to the Golgi and used again (Coutinho, Prata et al. 2012).

1.2.4. Protein reuptake through M6P receptors

Sometimes it may happen that lysosomal hydrolases escape the delivery pathway to lysosomes, ending up delivered outside the cell in the extracellular fluid. In that case, the escaped proteins are recognized by the CI-MPR, that has the ability to work on the cell surface. (Castonguay, Olson et al. 2011). Through this receptor, the enzyme is internalized and delivered to the lysosomes through the endosomal pathway.

1.3. Lysosomal storage disorders

An example of malfunctioning in the previously described pathway are lysosomal storage disorders (LSDs), a group of conditions inheritable by autosomic recessive traits, that results in faulty activity of lysosomes. They are caused by mutations inside the genomic sequence of several types of proteins involved in lysosomal activity, such as proteases, transporters, membrane proteins and activators. In most cases, these diseases cause an accumulation of the substrate of the mutated enzyme, leading to cell dysfunction and death (Platt, d'Azzo et al. 2018).

There are over 70 different diseases classified as LSDs with an incidence of 1 in 5000 live births, if we consider all the diseases as a group. The entity and progression of each LSD depend on the type of mutated protein its substrate. Some substrates, depending on their nature, are more prone to accumulate in some tissues or in some type of cells, leading to different rates of toxicity and tissue damage throughout the body. A good example is circulating monocytes and tissue macrophages, who are the most affected by LSDs being responsible for clearance of dead cells, leading to enhanced inflammation that contributes to disease progression (Rigante, Cipolla et al. 2017).

In the past decades several types of potential therapies have been found as potential candidates to improve the survivability and quality of life of

patients affected by LSDs. The most important are enzyme replacement therapies (ERT), to restore defective enzymes, or small-molecule therapies, where the production of over-stored substrates is inhibited, thus decreasing cellular stress (Platt, d'Azzo et al. 2018).

In general, this type of diseases has a manifestation that can start from birth to adulthood, depending on the type of mutation of the enzyme and how this influences enzyme activity (Sakai, Inui et al. 1994). Typical symptoms include ataxia, muscle weakness and mental deficits (Platt, d'Azzo et al. 2018).

1.3.1. Krabbe disease

This study will focus on one specific LSD, the Krabbe Disease (KD), caused by single mutations on several sites of the lysosomal enzyme galactosylceramidase, essential for the processing of galactosphingolipids and the maintenance of the myelin sheath. In many cases, missense mutations disrupt the protein folding process and the enzyme is retained in the ER. For this reason, GALC cannot process its substrates, causing an accumulation inside the cell with associated toxicity and subsequent apoptosis, especially of myelin-forming oligodendrocytes and Schwann cells of central and peripheral nervous system. Moreover, without the enzyme activity, the myelin sheath is severely compromised (Spratley and Deane 2016).

There are two possible manifestations of the KD, classified as infantile onset (85%-90% of patients) and adult onset (10%-15% of patients). In the infantile-onset disease, general symptoms are extreme irritability, spasticity and developmental delay before age 12 months, with the average age of death being 24 months, while symptoms in the adult-onset form are very variable depending on the residual activity of the enzyme, and they can present blindness, sensorimotor neuropathy and mental deterioration (Orsini, Escolar et al. 1993).

Regarding potential therapeutic approaches, the main challenge with KD is that the medication needs to cross the blood brain barrier (BBB) to be effective against the death of central nervous system (CNS) neurons. For other LSDs, such as Gaucher's, Fabry's and Pompe's diseases, ERT is an effective treatment, but for KD the recombinant enzymes are too big to cross the BBB (Spratley and Deane 2016). It has been proven that some viral vectors are able to cross the BBB for CNS delivery and they represent a promising strategy to develop treatments for KD, but further progress needs to be done to have a functioning treatment (Rafi, Rao et al. 2012).

1.4. Galactosylceramidase (GALC)

1.4.1. Function

Galactosylceramidase belongs to the group of lysosomal hydrolases. This enzyme is responsible for the hydrolysis of the galactose ester bonds of sphingolipids, such as galactocerebroside (**Fig. 1**, B) and galactosylsphingosine, to produce the main lipid components of the myelin sheath. Mutation in its sequence, as explained in the previous paragraph, can interfere with the folding process, resulting in the enzyme retention in the ER (Chen, Rafi et al. 1993). To function, GALC must be aided by other proteins called saposins (**Fig 1**, A). It has been proved that a lack of saposins can result in KD, because the enzyme cannot properly work without them (Spiegel, Bach et al. 2005). There are two hypotheses regarding the role of saposins during sphingolipids metabolism (Hill, Cook et al. 2018). The first model, called "solubiliser", consist in saposins extracting lipids from the lysosome membrane, delivering them to GALC for processing. In the other model, called "liftase", saposins enter the lipid bilayer of the lysosomal membrane causing a distortion and allowing GALC to extract lipids and process them.

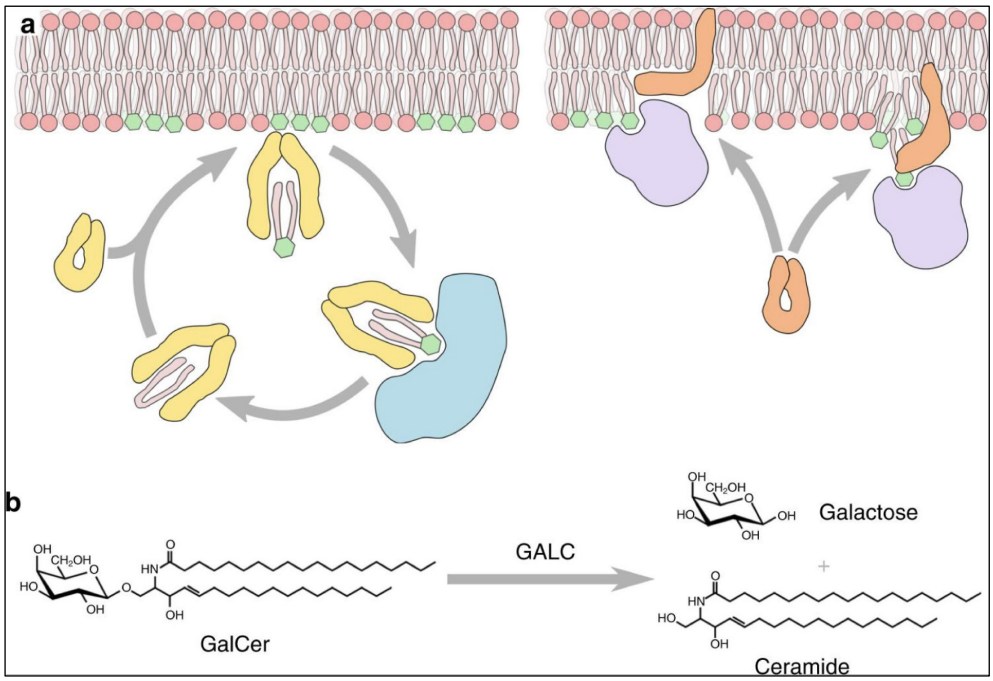

Figure 1: Glycosphingolipd processing by GALC (Hill, Cook et al. 2018)
A. Schematic representation of saposins (in yellow and orange) while assisting GALC in sphingolipds metabolism. On the left it is pictured the solubiliser model, where saposins extract lipids (green) from the bilayer. On the right it is pictured the liftase model, where saposins insert into the bilayer, creating a space for GALC to extract lipids.
B. Cleavage of galactocerebroside (GalCer) by GALC, producing galactose and ceramide.

1.4.2. Structure

GALC is synthesised as a unique polypeptide chain of 669 amino acids with a total weight of approximately 80 kDa (Nagano, Yamada et al. 1998). Once inside the acidic environment of the lysosome, the 80 kDa protein is cleaved into two subunits, one of 50 kDa (1-435 amino acid) and the other of 30 kDa (436-669 amino acid), the first one containing the N-terminal part of the protein, while the second one containing the C-terminal. Neither one of the two fragments express GALC activity taken alone, meaning that probably they are both needed for the final enzymatic structure and functioning (Nagano, Yamada et al. 1998).

The complete protein is made by three domains. The central domain is a triosephosphate isomerase (TIM) barrel, then there is a β-sandwich domain and a lectin domain, the last one being responsible for the binding with the galactose (Deane, Graham et al. 2011). In its sequence we can find six

potential N-glycosylation sites, being N127, N363, N387, N540, N543 and N586 (Sakai, Inui et al. 1994).

1.4.3. Maturation pathway

After the synthesis, GALC is co-translationally transported into the ER, where it undergoes its folding and glycosylation processes (Deane et al. 2011). In the Golgi apparatus N-glycans are modified by adding M6P groups, that will be recognized by the cation-independent M6P receptor and used by the translocation machinery to address GALC to lysosomes (Spratley and Deane 2016). GALC can take a different pathway to reach the lysosomes, by going through secretion and reuptake via M6P receptors on the outside of the cellular membrane (**Fig. 2**) (Nagano, Yamada et al. 1998). It has been shown that residual GALC activity influences the entity of the secretion outside the cell, showing no secretion for mutants completely inactive and little secretion for mutants with small residual activity (Lee, Kang et al. 2010). Probably the reason behind this is that only folding-competent GALC can leave the ER, so the secretion is proportional to the quantity of functioning enzyme inside the cell.

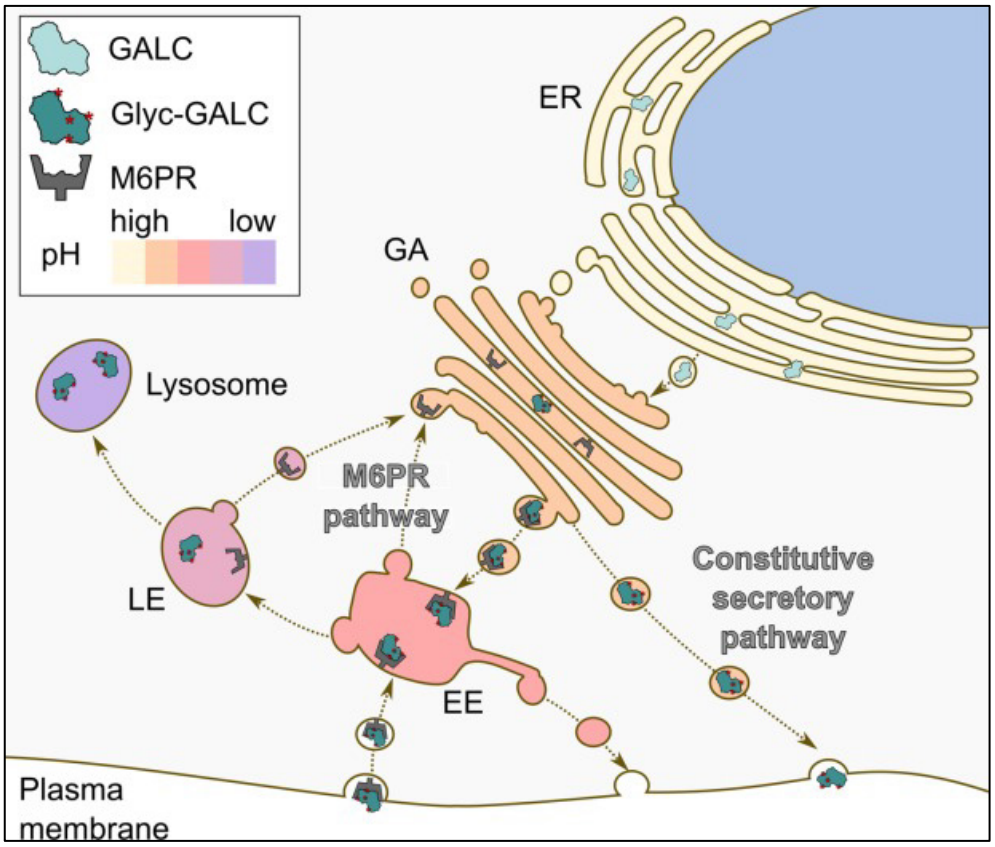

Figure 2: GALC maturation pathway (Spratley and Deane 2016)
GALC is co-traslationally translocated inside the ER, where it acquires its native structure and it is glycosylated. Then it passes through the Golgi, where its sugars are modified in more complex ones (Glyc-GALC) These glycans are recognized by M6P receptors and transported to early endosomes (EE). When the pH starts to become more acidic in late endosomes (LE), GALC dissociates from M6P receptors and it is delivered to lysosomes. GALC can also be secreted outside the cell and be internalized again via reuptake through M6P receptors on the cellular membrane.

1.4.4. Mutants analysed in this study

In this work, the wild type (WT) form of GALC and four different mutants are analysed: G41S, G270D, T513M, Y551S.

The mutants G41S, T513M and Y551S are shown to cause the infantile onset of the disease, having a residual activity basically close to zero (Wenger, Rafi et al. 1997)(Spratley and Deane 2016). The mutant G270D is responsible for a less severe, adult-onset form of the disease, showing some residual activity and secretion outside the cell (Nagano, Yamada et al. 1998)(Hossain, Otomo et al. 2014).

2. AIM OF THIS WORK

The aim of this work is to study the biogenesis and lysosomal transport of the wild-type form of GALC, and of four folding-defective GALC mutants (G41S, G270D, T513M, Y551S) responsible for the Krabbe disease. The investigation is performed in mammalian cultured cells, which are transiently transfected for expression of the five model polypeptides, whose intracellular fate will be monitored by biochemical and indirect immunofluorescence techniques. Generation of a cell model that recapitulates the diseases phenotype (i.e., the wild type GALC is delivered to the lysosomal compartments, whereas mutant GALC is retained in the ER and possibly degraded), would allow the screening of pharmacological chaperones. These molecules, when administered to patients, should assist/enhance the correct folding and lysosomal trafficking of mutant forms of GALC, thereby re-establishing their physiologic function.

3. MATERIALS AND METHODS

3.1. Molecular biology

3.1.1. Plasmid design

A total of five plasmids were designed using the software SnapGene™, one for each version of the protein studied in this work. The wild-type sequence of the protein was modified adding mutations (one for each variant), restriction sites and linkers. Then each construct was inserted into a pCDNA3.1(+) plasmid and their sequence were sent to GenScript for DNA synthesis and amplification.

3.1.2. DNA quantification

Samples of plasmid DNA were quantified using Nanodrop 2000c/2000 UV-Vis Spectrophotometers. To measure the DNA concentration, 1 µl is taken and placed on the reader, which gives back the concentration in ng/µl.

3.2. Cell biology

3.2.1. Cell lines and culture medium

Human embryonic kidney 293 (HEK293) and mouse embryonic fibroblasts (MEF) cells were grown in DMEM medium, with the addition of 10% foetal bovine serum (FBS). Culture conditions were 37 ^{o}C and 5% CO_2.

3.2.2. Cell culture

Cells were cultured in 10 cm Petri dishes and splitted in new dishes at least two times per week, after they reached at least 80% confluence.

To perform the cell passage, the old medium was removed, the cells were washed with PBS and incubated with 1 ml of trypsin for 5 minutes. After the

complete detachment from the old dish, cells were transferred at the appropriate concentrations in new dishes with fresh medium.

3.2.3. Cell counting

Cells were counted before passage and seeding procedures using a CellDrop™ automatic cell counter (DeNovix®). For each counting, 10 µl of cell solution was injected into the capillary and used to count the number of cells present in 1 ml.

3.2.4. Transient transfection of mammalian cells

To perform protein biochemistry, 5 million HEK293 cells were seeded in 6 cm dishes. After 8 hours, cells were transfected with 1,5 µg of plasmid DNA per dish.

The appropriate volume of DNA was diluted into 300 µl of JetPrime™ buffer and 3 µl of JetPrime™, incubated 10 minutes at room temperature and then applied onto the dishes in the form of drops. After 21 hours of incubation, the cells were lysed and the PNS was taken for analysis.

To perform indirect immunofluorescence, 150.000 MEF cells were seeded in each well of 12 multi-well plates, containing microscope coverslips coated in Alcian blue. After 8 hours, cells were transfected with 1 µg of plasmid DNA per dish. The appropriate volume of DNA was diluted into 100 µl of JetPrime™ buffer and 2 µl of JetPrime™, incubated 10 minutes at room temperature and then applied onto the wells in the form of drops. After 16 hours of incubation, the cells were fixated in paraformaldehyde 10% and prepared for confocal microscopy.

3.3. Protein biochemistry

3.3.1. Cell lysis

HEK293 cells were washed with a solution of phosphate buffer saline (PBS) and N-ethylmaleimide (NEM) 20 mM for 1 minute. Then they were lysed with a solution of RIPA buffer (1% triton, 0.1% SDS, 0.5% sodium-deoxycholate in HBS, pH 7.4) with the addition of proteases inhibitors. Cells were incubated with the lysis buffer for 20 minutes and then the PNS was collected by centrifugation at 4 ^{o}C and 10000g for 10 minutes, to separate it from the nuclei. The PNS was analysed through SDS-PAGE or immunoprecipitation.

3.3.2. SDS-page and Western blot analysis

Proteins were analysed through SDS-PAGE using a 10% SDS bis-acrylamide gel under reducing conditions, mixing samples with dithiothreitol (DTT) and sample buffer. Samples were boiled at 95 ^{o}C for 5 minutes before loading into the gel. After the run, proteins are transferred into a PVDF membrane using the TransBlot Turbo transfer system (BioRad). The membrane is blocked using 8% (w/v) skimmed dry-milk and then incubated with primary and HRP-conjugated secondary antibodies. Membrane development is done using WesternBright ECL Kit (Adrensta) and the detection of the HRP signal is done through the FusionFX system.

3.3.3. Immunoprecipitation of the protein of interest

Cellular lysate samples were incubated for 2-4 hours at 4 ^{o}C with protein A beads and an anti-HA specific antibody to immunoprecipitate against the HA tag. For the V5 tag, samples were incubated with agarose beads conjugated through a disulphide bridge with an anti-V5 antibody.

After the incubation, samples were washed with RIPA lysis buffer for two times. Samples with anti-HA antibodies were directly boiled with sample

buffer at 95 ^{o}C before loading them into the gel, while samples with anti-V5 conjugated beads were firstly separated from the beads, and then boiled with sample buffer. After the boiling, samples were analysed through SDS-PAGE and Western blot.

3.4. Indirect immunofluorescence

Cells were seeded on glass coverslip coated with alcian blue and left to grow for 17 hours. Then they were washed with PBS and fixed using a solution of paraformaldehyde 3.7%. Coverslips were subsequently permeabilised with a solution of 10% goat serum, 15 mM Glycine, 0.05% saponin and 10 mM Hepes and treated with primary and secondary antibodies. Antibodies were diluted using the permeabilization solution and incubated with coverslips, respectively 3 hours for the primary and 1 hour for the secondary. Images were acquired using a confocal laser scanning microscope (LEICA DI600, SP5 scan head, HCX PL APO CS 63X oil UV objective).

Antibodies used in this work

Name/Specificity	Species	Dilution	Supplier/source
Primary antibodies			
anti-HA	rabbit	WB: 1:3000	Sigma
anti-V5	mouse	WB: 1:5000 IF: 1:100	Abcam
anti-LAMP1	rat	IF: 1:50	Hybridoma 1D4B
Secondary antibodies			
protein A-HRP		WB: 1:20000	Invitrogen
anti-mouse-HRP	goat	WB: 1:20000	SouthernBiotech
anti-rat IgG Alexa 647	goat	IF: 1:300	SouthernBiotech
anti-mouse IgG Alexa 568	goat	IF: 1:300	SouthernBiotech

4. RESULTS

4.1. Molecular biology

The first step for the study of GALC wild-type and its four mutants was the design of constructs to transiently express the proteins of interest in HEK293 and MEF cells. Five different constructs were designed using SnapGene™, one for the wild-type form and four folding-defective variants. The coding sequence used for the wild type was taken from UniProt (P54803) and corresponds to the human form of GALC. The methionine in position 17 is considered as the start codon (Sakai, Inui et al. 1994). For the G41S mutant, a glycine in position 41 was changed with a serine (GGC→AGC). For the G270D mutant, a glycine in position 270 was changed with an aspartic acid (GGC→GAC). For the T513M mutant, a threonine in position 513 was changed with a methionine (ACG→ATG). For the Y551S mutant, a tyrosine in position 551 was changed with a serine (TAC→TCC).

4.1.1. Constructs design

The coding sequence of GALC was inserted into a pCDNA3.1 (+) plasmid (**Fig. 3B**). The insert was placed downstream the cytomegalovirus promoter, which ensures an efficient and abundant protein production, using AflII and XhoI as restriction sites on the extremities of the plasmid insert. Besides GALC coding sequence, other elements were included in the plasmid insert. The prolactin signal sequence was inserted upstream the coding sequence to allow efficient ER translocation of newly synthesised GALC. The Kozak sequence is needed for the recognition of the RNA by the complex responsible for protein synthesis (**Fig. 3A**). As mentioned previously in the Introduction, in the section explaining GALC structure (1.4.2), an important step in the maturation process is the cleavage of the 80 kDa protein in two subunits of 50 and 30 kDa. To monitor the maturation of GALC, two different tags were added at the N and C terminal of the protein, respectively an HA

tag and a V5 tag (**Fig. 3A**). In this way we could detect the presence of the complete protein using both tags, or selectively look at the presence of the 50 or 30 kDa subunits with two different antibodies. The presence of the fragment is an indication of a successful synthesis and trafficking of the enzyme to the lysosome.

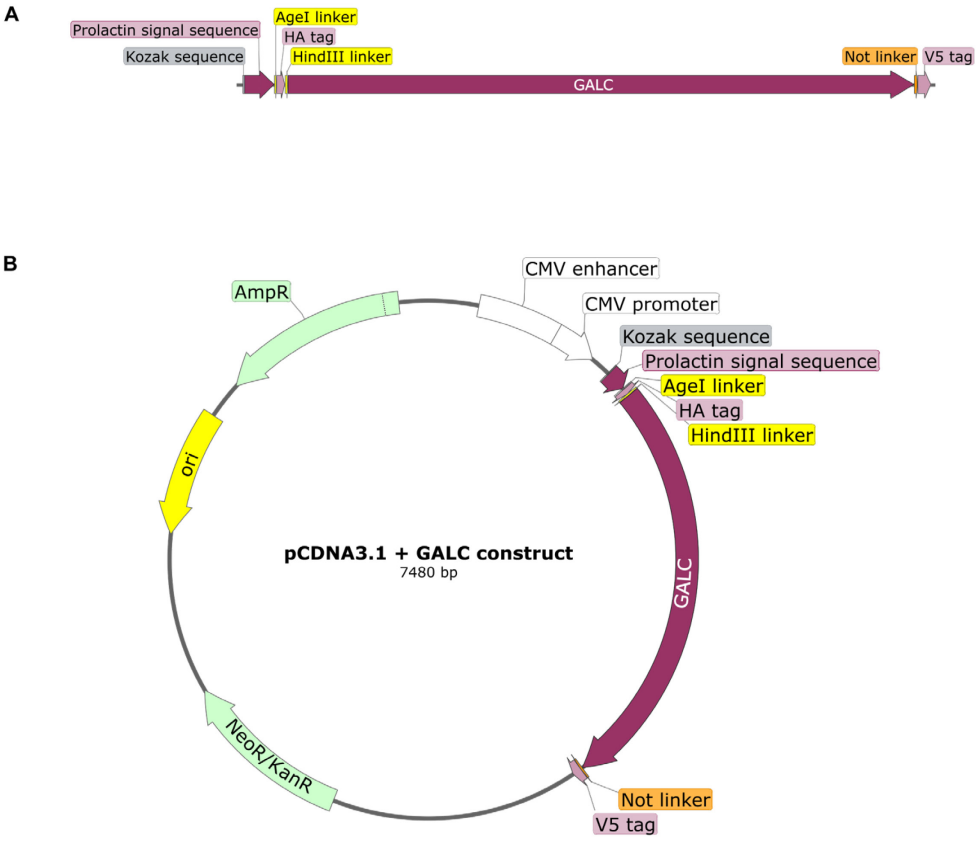

Figure 3: Constructs design
A. Schematic of the plasmid insert for GALC expression. In the map the GALC gene is tagged with the HA-tag on the N-terminal end, while it is tagged with the V5-tag on the C-terminal end. There are also represented the linkers in between different components of the insert, the Kozak sequence and the prolactin signal sequence.
B. Schematic of the complete plasmid with the GALC insert. In the plasmid map are highlighted the most important genes: the origin of replication (*ori*), the antibiotic resistance genes for positive selection in the presence of Ampicillin, Neomycin or Kanamycin and the cytomegalovirus promoter.

This procedure was made with SnapGene™ and the complete sequence was sent to GenScript for the synthesis and amplification of our construct.

4.2. Biochemistry

4.2.1. Expression of GALC variants in mammalian cells

The first step in the characterization of GALC maturation was the transfection of HEK293 cells with the pCDNA3.1 constructs encoding for the protein, as described in Material and Methods section (3.2.4). Cells were transfected with an empty pCDNA3.1 (**Fig. 4 A-B**, lane 1), GALC WT and the four different mutants (**Fig. 4 A-B**, lanes 2-6). The WT form of the protein is meant to be used as a reference, to allow comparison with folding-defective mutants, while the mock-transfected sample was essential to exclude possible cross reactions of anti-HA and anti-V5 antibodies used for the WB with other proteins present in cell lysates. 21h after transfection, cells were lysed with a RIPA buffer (Materials and Methods, 3.3.1). Cellular lysate was centrifuged and the PNS was separated from the nuclei. Then 10 µl of cellular lysate were subjected to SDS-page under reducing conditions. Proteins were then transferred into PVDF membranes and analysed through Western blot analysis using anti-HA (**Fig. 4A**) or anti-V5 (**Fig. 4B**) antibodies.

The antibody anti-HA tag did not detect any signal on the membrane, while the one with anti-V5 antibody highlighted a single line of protein bands between the 97 kDa and 66 kDa molecular weight markers (**Fig.4B**, lanes 2-6). GALC molecular weight is around 80 kDa, corresponding to the highlighted bands. The absence of signal in the mock-transfected sample (**Fig. 4B**, lane 1), confirm the specificity of the anti-V5 antibody in the recognition of GALC variants.

Our hypothesis, regarding the inability to see any kind of protein in the anti-HA immunoblot (**Fig. 4A**), was that the tag could had been removed during GALC maturation or that the antibody-tag combination was not efficient in the recognition process, due to the low quantity of protein present in the membrane. Another reason could be that the N-terminal part of the protein

is buried in the 3-dimensional structure of the enzyme, making it difficult for the antibody to recognize properly the tag and mark it for WB.

Lastly, we were unable to detect the 30 kDa fragment, which should be present in the WB anti-V5 in lanes corresponding to the WT and G270D mutant (**Fig. 4B**, lanes 2 and 4). It is important to remember that this last mutant is partially functional and should undergo maturation like the WT, but on a lesser extent. Even if the anti-V5 antibody is more efficient in the recognition of the protein than the anti-HA one, we could not detect the 30 kDa fragment. The quantity of protein is too low, making it challenging to detect the fragment analysing only 10 µl of TCE.

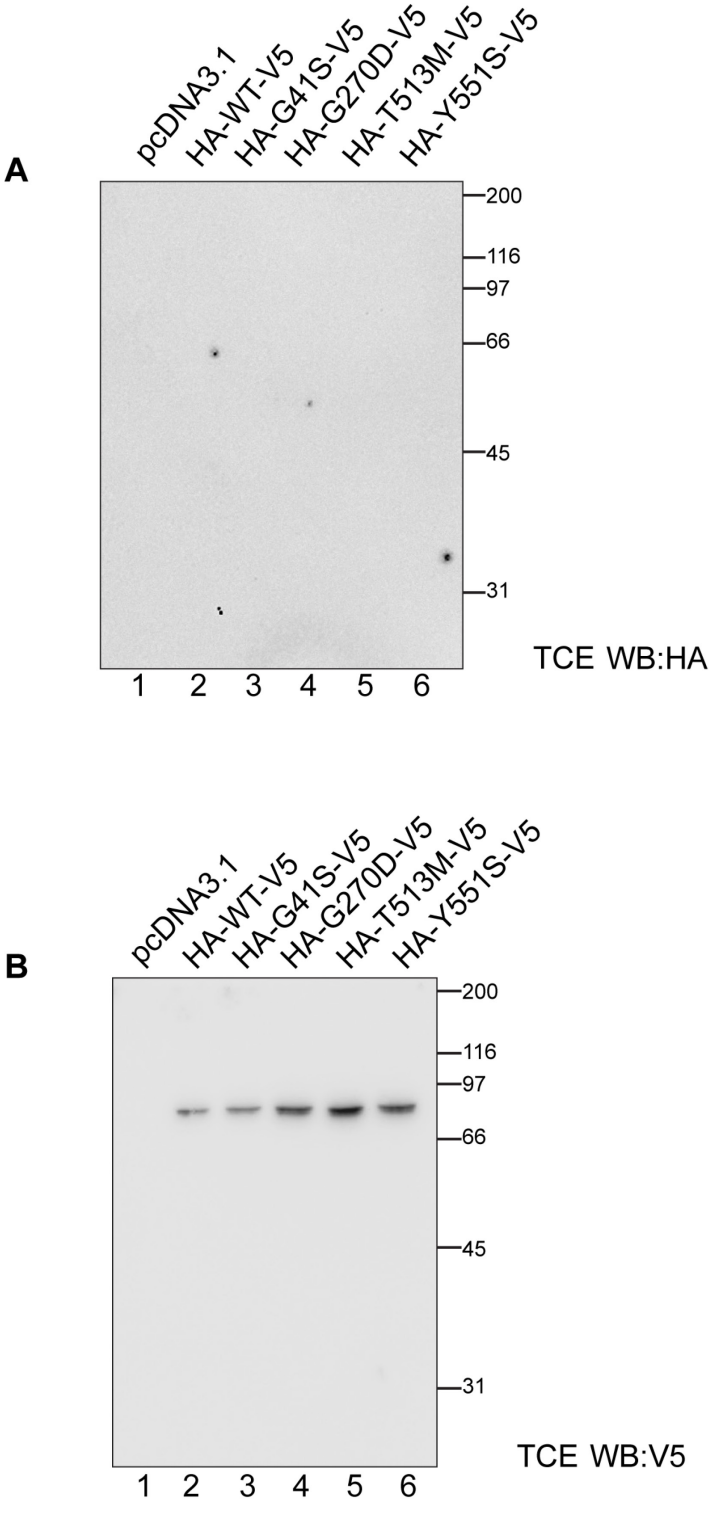

Figure 4: Expression of GALC variants in mammalian cells
A. HEK293 cells were transfected with pCDNA3.1 plasmids encoding for GALC WT (lane 2), G41S mutant (lane 3), G270D mutant (lane 4), T513M mutant (lane 5), Y551S mutant (lane 6). The first sample was transfected with an empty pCDNA3.1 plasmid for control purposes (lane 1). Western blot analysis was performed using an anti-HA tag antibody.
B. HEK293 cells were transfected with pCDNA3.1 plasmids encoding for GALC WT (lane 2), G41S mutant (lane 3), G270D mutant (lane 4), T513M mutant (lane 5), Y551S mutant (lane 6). The first sample was transfected with an empty pCDNA3.1 plasmid for control purposes (lane 1). Western blot analysis was performed using an anti-V5 tag antibody.

4.2.2. Cellular lysate immunoprecipitation and WB analysis

A solution to overcome the problems previously described (low antibody efficacy and low protein quantity) was found with the immunoprecipitation of the samples. This technique allows to enrich the protein of interest in analysed samples, making it more likely to be detected when subjected to Western blot. Cells were transfected and lysed in the same conditions described to perform TCE analysis through Western blot (4.2.1). After the lysis, two sets of 200 µl cellular lysate samples were subjected to immunoprecipitation, one against the HA tag and one against the V5 tag.

Analysis through Western blot revealed two identical sets of protein bands on both membranes (**Fig. 5** A-B). Unlike the WB analysis with 10 µl of TCE, we were able to detect the protein of interest also using the anti-HA antibody. The observed pattern of bands found after immunoprecipitation (**Fig.5** A-B, lanes 2-6) is the same observed in the WB analysis of the TCE (**Fig. 5B**, lanes 2-6). By looking at bands intensity, we can observe an important enrichment in protein quantity, being more evident in the anti-V5 immunoprecipitated WB (**Fig. 5B**, lanes 2-6) with respect to the anti-HA immunoprecipitated WB (**Fig. 5A**, lanes 2-6). This could be a confirmation of our previous hypothesis: the antibody used to recognize the HA tag, used both for immunoprecipitation and for WB, is probably less efficient than the anti-V5 antibody, resulting in the inability to see any results in the anti-HA TCE WB (**Fig. 5A**) and reduced protein quantity after IP (**Fig.5A** vs **Fig. 5B**). The 50 kDa and 30 kDa fragments were not detected. The inability to detect GALC fragments could be found in the last maturation step, which occurs inside the lysosomes. In the last stage of the maturation process happening in lysosomes, which generates the two subunits, probably also the terminal ends of the sequence are removed, resulting in the inability to see the fragments singularly.

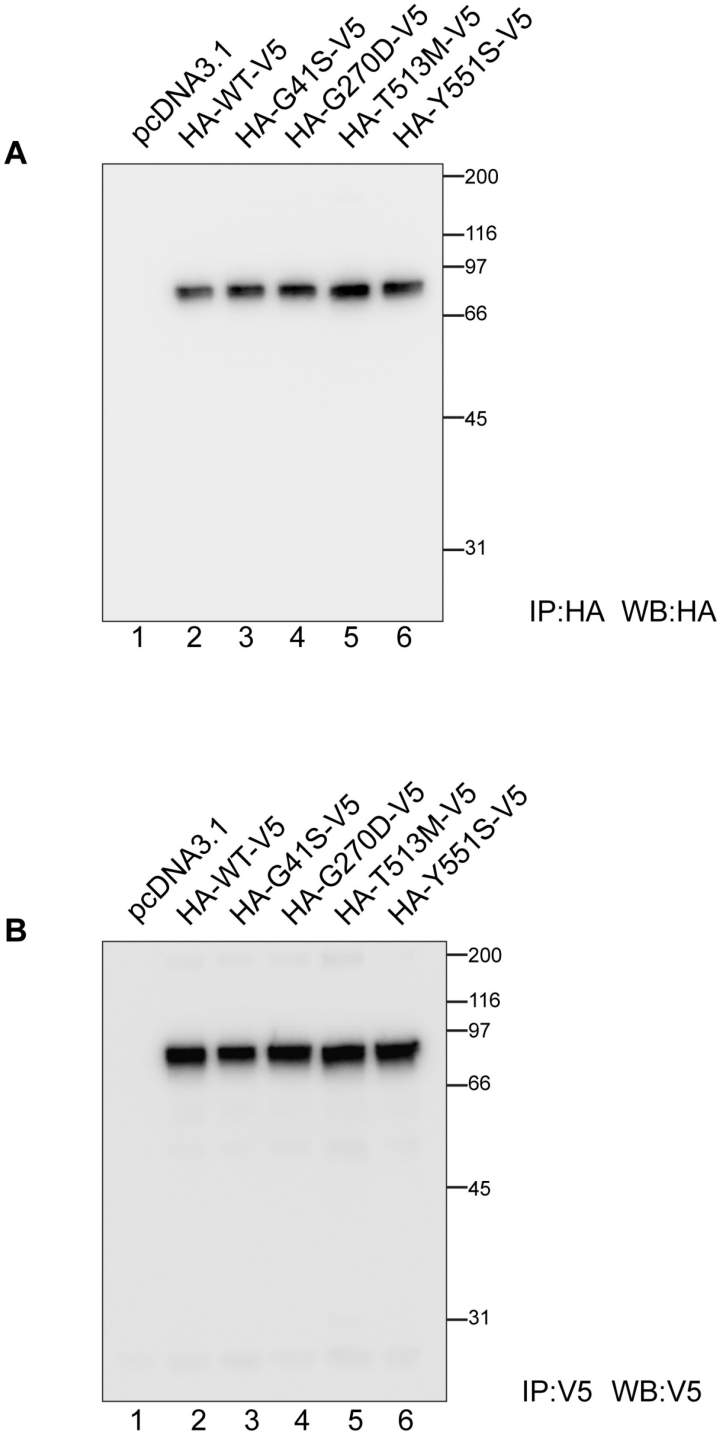

Figure 5: WB of immunoprecipitated cellular lysate samples
A. HEK293 cells were transfected with pCDNA3.1 plasmids encoding for GALC WT (lane 2), G41S mutant (lane 3), G270D mutant (lane 4), T513M mutant (lane 5), Y551S mutant (lane 6). The first sample was transfected with an empty pCDNA3.1 plasmid for control purposes (lane 1). After the lysis, samples were subjected to immunoprecipitation anti-HA. Western blot analysis was performed using an anti-HA tag antibody.
B. HEK293 cells were transfected with pCDNA3.1 plasmids encoding for GALC WT (lane 2), G41S mutant (lane 3), G270D mutant (lane 4), T513M mutant (lane 5), Y551S mutant (lane 6). The first sample was transfected with an empty pCDNA3.1 plasmid for control purposes (lane 1). After the lysis, samples were subjected to immunoprecipitation anti-V5. Western blot analysis was performed using an anti-V5 tag antibody.

4.2.3. GALC detection in cellular culture media

Because of the inability to detect GALC fragments in the cellular lysate, we decided to try another approach to evaluate the maturation and trafficking of the protein. We opted to analyse the cellular culture media to see if GALC was present as a cellular secretion product: if GALC is secreted, it means that the protein has successfully completed its maturation steps in the ER and in the Golgi, being also an indication of a functional enzyme (Introduction 1.4.3).

Cells were transfected in the same conditions described previously (4.2.1) and after 16 hours of incubation, cell culture media was removed and analysed. Two sets of 800 µl culture media samples were subjected to IP anti-HA and anti-V5 tags and analysed through WB.

WB analysis did not detect any proteins in the membrane treated with the anti-HA antibody (**Fig. 6A**). Conversely, anti-V5 antibody revealed secretion of GALC WT (**Fig. 6B**, lane 2) and G270D variant (**Fig. 6B**, lane 4). This is consistent with what we knew from papers (Spratley and Deane 2016), GALC variants expressing a folding competent protein are secreted (WT, G270D), while folding-defective mutants are retained inside the ER and are not found in the cellular culture media (G41S, T513M, Y551S). It is important to mention also the difference in quantity of protein secreted between the WT form of the enzyme and the partially folding-competent variant G270D: the mutation probably causes a partial retention inside the ER, with only a portion of the total protein passing the cellular controls and being secreted (**Fig. 6B**, lane 2 vs lane 4). The inability to detect any proteins with the anti-HA antibody could be due to low antibody efficacy in recognizing the HA tag on GALC, which is only detected using the more sensitive anti-V5 antibody. Another reason could be found in the maturation processes through the Golgi: complex sugars could be interfering with the recognition of the HA epitope, hiding it from the antibodies used for IP and WB.

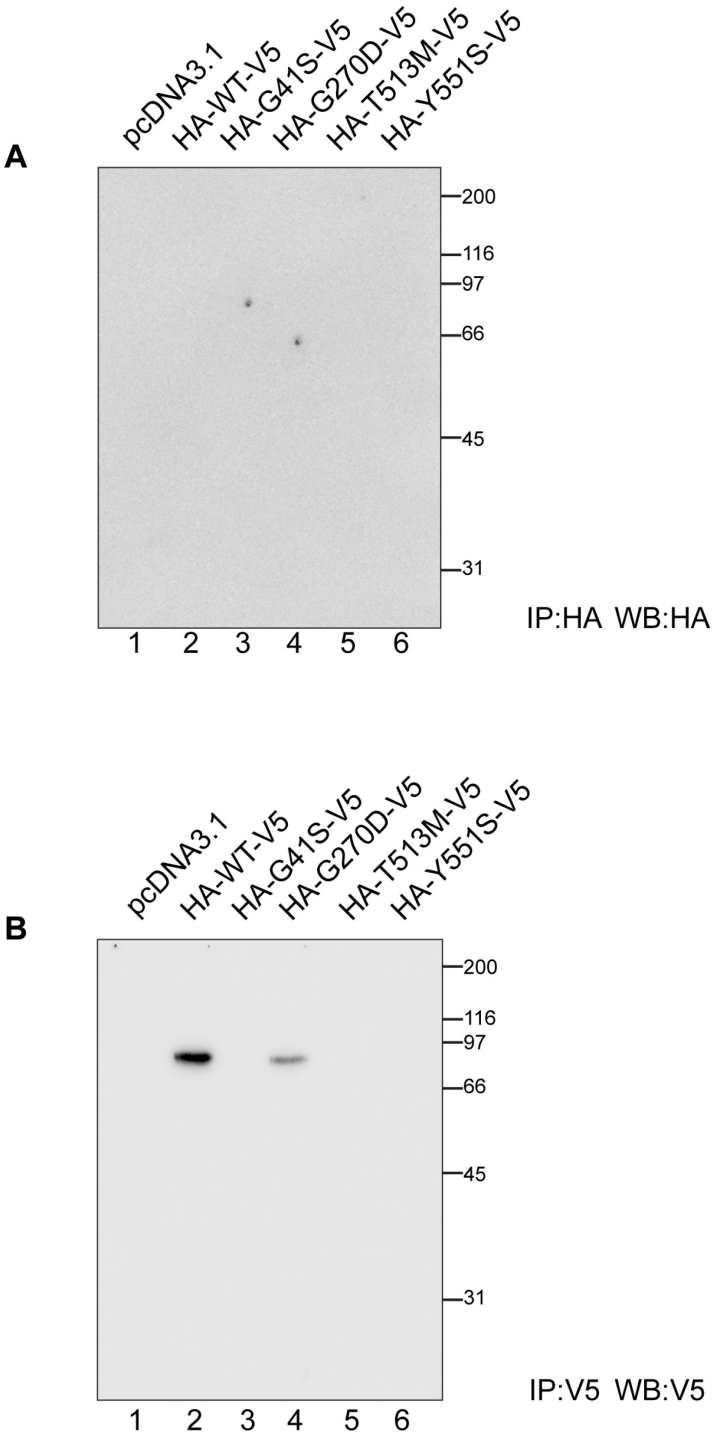

Figure 6: Cellular culture media WB analysis, after IP
A. HEK293 cells were transfected with pCDNA3.1 plasmids encoding for GALC WT (lane 2), G41S mutant (lane 3), G270D mutant (lane 4), T513M mutant (lane 5), Y551S mutant (lane 6). The first sample was transfected with an empty pCDNA3.1 plasmid for control purposes (lane 1). 800 µl of cellular culture media was subjected to immunoprecipitation anti-HA. Western blot analysis was performed using an anti-HA tag antibody.
B. HEK293 cells were transfected with pCDNA3.1 plasmids encoding for GALC WT (lane 2), G41S mutant (lane 3), G270D mutant (lane 4), T513M mutant (lane 5), Y551S mutant (lane 6). The first sample was transfected with an empty pCDNA3.1 plasmid for control purposes (lane 1). 800 µl of cellular culture media was subjected to immunoprecipitation anti-V5. Western blot analysis was performed using an anti-V5 tag antibody.

4.2.4. Endoglycosidase H (EndoH) assay

After assessing GALC secretion in the cellular media of folding-competent variants, we decided to test also the glycosylation of the protein through a biochemical assay using Endoglycosidase H. This enzyme allows to distinguish from protein that are retained in the ER and protein that complete their maturation process through the Golgi: when proteins pass through the Golgi their sugars are modified, becoming more complex and resistant to EndoH cleavage (**Fig. 7**). Since GALC is glycosylated on six N residues inside the ER, it can be useful to confirm if the secreted protein found in the cellular culture media is the mature form, after passing through the Golgi and being subjected to sugars modification (Introduction, 1.2.4). Cellular lysate was also treated with Bafilomicyn A1 (BafA1), which is a proton pump inhibitor that blocks lysosomal activity. BafA1 treatment prevents GALC maturation in the lysosome (Introduction, 1.4.2). For this assay we decided to perform IP and WB analysis only with anti-V5 antibodies.

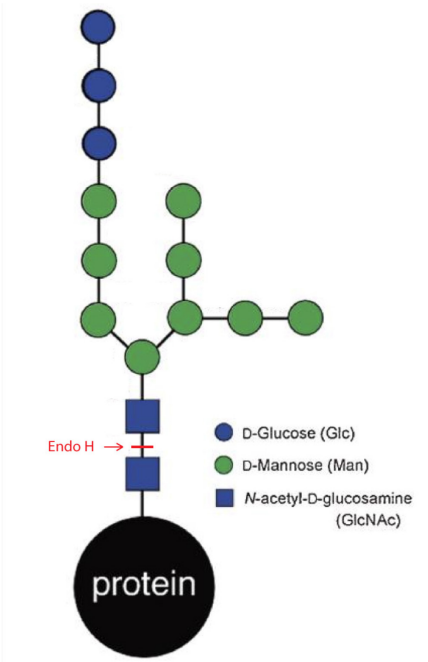

Figure 7: EndoH cut on N-glycosylated proteins (Ito and Takeda 2012)
Schematic on the cutting site of EndoH on ER N-glycosylated proteins (in red)

For the EndoH assay on GALC recovered from cellular culture media, cells were transfected in the same conditions described previously (4.2.1) and after 16 hours of incubation, 800 µl of cell culture media was removed, subjected to anti-V5 IP and analysed through WB. For the EndoH on cellular lysate, 21h after transfection, cells were lysed with a RIPA buffer (Materials and Methods, 3.3.1). Cellular lysate was centrifuged and the PNS was

separated from the nuclei. Then 200 µl of cellular lysate were subjected to anti-V5 IP and analysed through WB.

Analysis from the WB showed an overall sensitivity of glycosylated GALC to EndoH in the cellular lysate samples (**Fig.8A**), indicating that the recovered protein is mostly the ER retained GALC. Meanwhile, GALC recovered from the cellular culture media showed resistance to EndoH treatment (**Fig. 8B**), especially if compared to the shift in MW present in proteins from cellular lysate (**Fig. 8B** vs **Fig. 8A**). This confirmed that the secreted protein had indeed passed through the Golgi having its sugars modified, becoming resistant to enzymatic cut by EndoH. Lanes corresponding to the BafA1 treatment showed increased intensity with respect to the untreated lanes, due to increased protein quantity inside the cell caused by lysosomal inactivity.

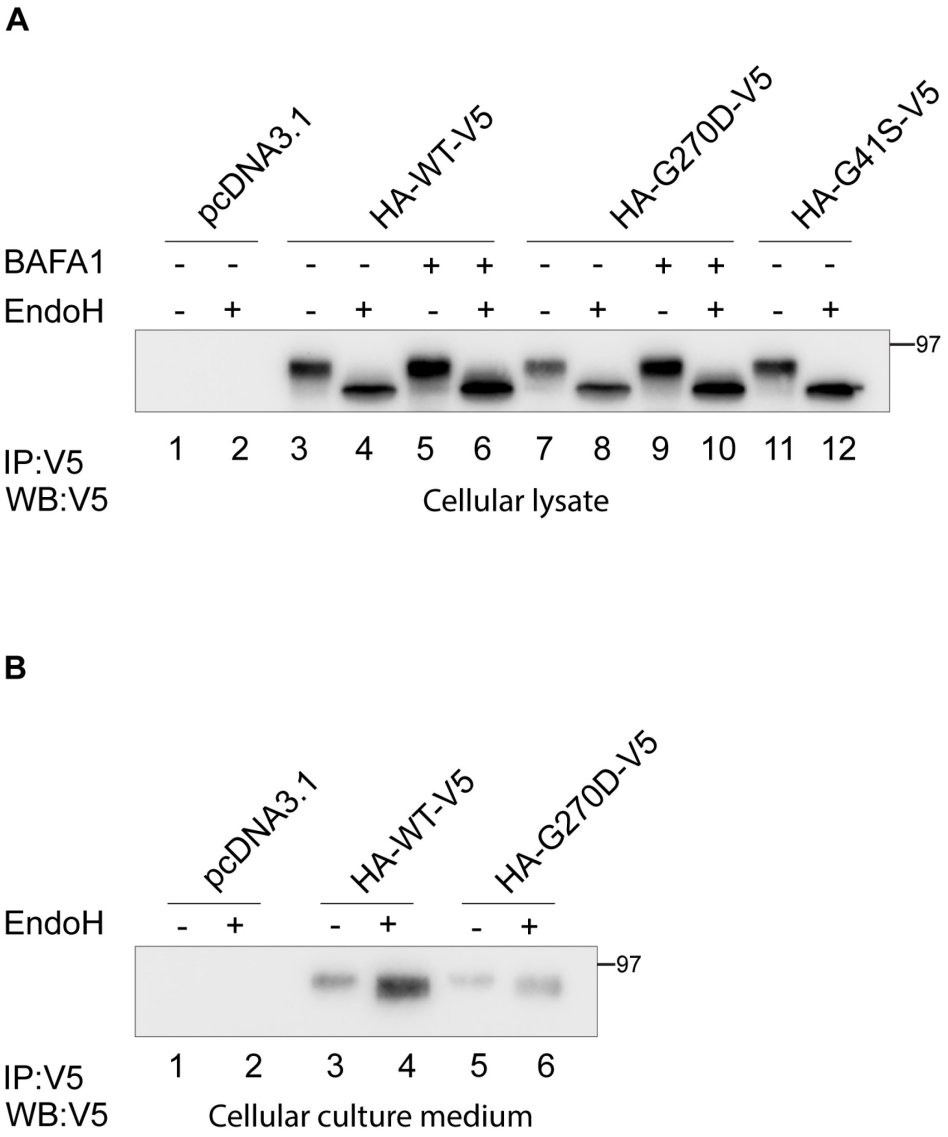

Figure 8: Endoglycosidase H treatment of cellular lysate and cellular culture media after IP
A. HEK293 cells were transfected with pCDNA3.1 plasmids encoding for GALC WT (lanes 3,4,5,6), G41S mutant (lanes 11,12), G270D mutant (lanes 7,8,9,10) and an empty pCDNA3.1 plasmid for control purposes (lanes 1,2). 200 µl of cellular lysate were subjected to immunoprecipitation anti-V5 and treated with EndoH. Western blot analysis was performed using an anti-V5 tag antibody.
B. HEK293 cells were transfected with pCDNA3.1 plasmids encoding for GALC WT (lanes 3,4), G270D mutant (lanes 5,6) and an empty pCDNA3.1 plasmid for control purposes (lanes 1,2). 800 µl of cellular culture media was subjected to immunoprecipitation anti-V5 and treated with EndoH. Western blot analysis was performed using an anti-V5 tag antibody.

We also noticed different intensities between the bands of secreted WT and G270D with and without EndoH, being more evident in the WT (**Fig. 8B**, lanes 3 vs 4, lanes 5 vs 6). A minor shift was also observed comparing EndoH treated and untreated lanes for each GALC variant. Our hypothesis was that not all six sugars were modified in the Golgi, leading to some of them still

being cut by EndoH. This partial cut could be the reason for the minor smearing observed in the EndoH treated bands (**Fig. 8B**, lanes 4 and 6) and for their increased intensity. If one or two sugars are cut, they could uncover key parts of the epitope recognized by the antibody used for WB, improving the binding affinity and detection of the protein embedded in the membrane.

4.3. Indirect immunofluorescence and confocal microscopy

To assess the intracellular localisation of GALC WT and its mutants, we performed confocal laser scanning microscopy. Cells were seeded on alcian-blue stained coverslips, transfected with the plasmids coding for GALC variants and treated with BafA1. Cells were then fixed, permeabilised with a saponin solution (Materials and methods 3.4), stained with the anti-V5 antibody to detect GALC and with an anti-LAMP1 antibody, a typical lysosomal marker (Materials and methods 3.4).

4.3.1. Intracellular localisation of GALC variants

The anti-V5 antibody showed that GALC localized in the lysosomes only in the WT and G270D variants (**Fig. 9**, Inset A-C). These results confirm what we were expecting: folding-competent mutants (WT, G270D) pass the ER quality control machinery and are delivered to lysosomes, while folding-defective mutants are retained into the ER and cannot be seen inside lysosomes (**Fig. 9**, Inset B-D-E). By comparing the WT and G270D variants, at first glance we can also notice a difference in quantity of delivered protein to lysosomes (**Fig. 9**, Insets A vs C), confirming that the mutant is only partially folding-competent, causing a lower delivery than the WT.

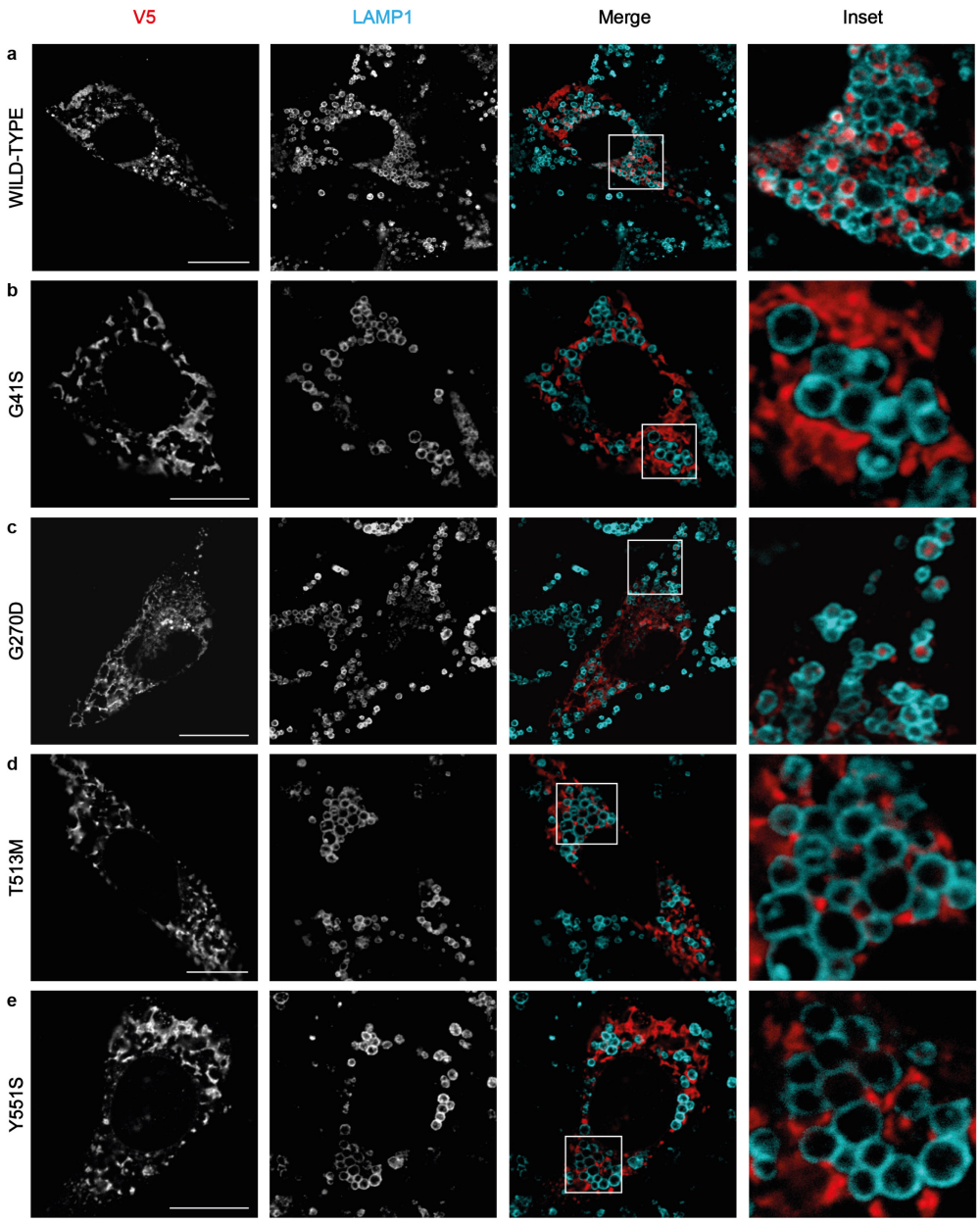

Figure 9: Intracellular localisation of GALC variants in MEF cells
MEF cells were transfected with pCDNA3.1 plasmids encoding for GALC WT (lane A), G41S mutant (lane B), G270D mutant (lane C), T513M mutant (lane D), Y551S mutant (lane E). Cells were fixed, permeabilised and stained with the anti-V5 antibody and an anti-LAMP1 antibody. Merge panels show co-localisation of GALC and lysosomes, with a magnification showed in Inset panels.

4.3.2. Quantification of loaded lysosomes through LysoQuant

To quantify the lysosomal delivery of GALC WT and folding-defective variants, we analysed the pictures obtained with the confocal microscope with an informatic tool called LysoQuant. This tool exploits a deep-learning

approach for segmentation and classification of fluorescence images capturing cargo delivery within endolysosomes for clearance, allowing to distinguish loaded and empty lysosomes (Morone et al. 2020).

Ten pictures for each GALC variant were analysed with LysoQuant. After the analysis, this tool outputs the number of empty, loaded and total lysosomes. It is important to mention that LysoQuant does not distinguish between different quantities of cargo in loaded lysosomes, classifying them equally as loaded. We proceeded to calculate the percentage of loaded lysosomes on the total number detected by LysoQuant and we plotted the results in a histogram (**Fig. 10**). The data were also analysed through an Anova test, represented in the plot with black asterisks. The results are a confirmation of what we observed at the confocal microscope. The WT is the variant most abundantly delivered to lysosomes, as we expected, since it was the reference value for a completely functional enzyme (**Fig. 10**, WT). The G270D variant is delivered on a lower level if compared to the WT, as we expected since it is responsible for a mild form of the disease and the enzyme is partially capable of folding, but still retained in the ER to some extent (**Fig. 10**, 270 vs WT). The other variants (G41S, T513M, Y551S) have a significantly lower delivery if compared to the WT and the 270 variants, as expected since they are completely folding-defective. By looking at the plot, we can see that there is a discrepancy between what we can observe by eye in the panels obtained at the confocal microscope (**Fig. 9**) and the plot with LysoQuant results. In the panels the three fully folding-defective variants (**Fig. 9**, lanes B-D-E) cannot be found inside any of the lysosomes, but when we observe data obtained with LysoQuant we find a lower percentage of delivery, as we can see from scattered black dots in the histogram (**Fig. 10**, 41-513-551). We need to remember that LysoQuant is not totally accurate when recognizing loaded lysosomes: it may happen that the programme detects a very weak signal inside the lysosome and, even if it is due to an unspecific binding of the antibody, lysosomes are classified as loaded. Moreover, lysosomes do

not all have a perfectly circular edge or clear shape, sometimes they are stacked on each other and it can be difficult for LysoQuant to perform a totally accurate distinction of loaded and empty lysosomes.

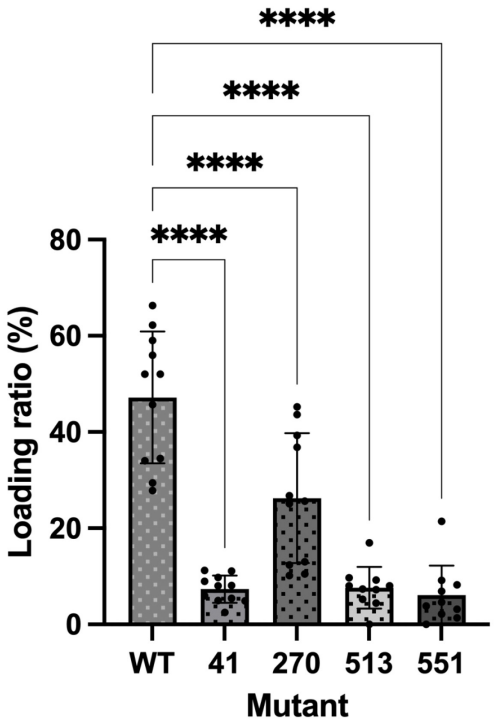

Figure 10: Lysosomal loading ratio of GALC variants in MEF cells
MEF cells were transfected with pCDNA3.1 plasmids encoding for GALC WT, G41S mutant, G270D mutant, T513M mutant, Y551S mutant. Cells were fixed, permeabilised and stained with the anti-V5 antibody and an anti-LAMP1 antibody. After that they were analysed with the confocal microscope and 10 pictures from each variant were subjected to LysoQuant analysis.

5. DISCUSSION

Galactosylceramidase (GALC) is a lysosomal hydrolase responsible for sphingolipids metabolism, ensuring a proper maintenance of the nervous myelin sheath. Folding-defective mutants of GALC are unable to pass the ER quality control machinery, resulting in accumulation of misfolded proteins inside the in the ER and in the accumulation of toxic intermediates inside the CNS cells, causing their premature death. Moreover, the absence of a functional enzyme causes a demyelization of the CNS nerves. The resulting pathology is called Krabbe disease, classified among the lysosomal storage disorders (LSD) (Chen, Rafi et al. 1993).

In this work we studied the wild-type form of the enzyme, plus four mutants: G41S, G270D, T513M, Y551S. The G270D variant is responsible for a mild, adult-onset form of the disease (Nagano, Yamada et al. 1998)(Hossain, Otomo et al. 2014). Conversely, the G41S, T513M and Y551S variants are responsible for a more severe, child-onset form of the disease (Wenger, Rafi et al. 1997)(Spratley and Deane 2016).

We characterized GALC WT and its mutants in mammalian cells with biochemistry and indirect immunofluorescence techniques. Our results show that folding-competent variants of GALC are secreted outside the cell and the secretion is correlated to the folding efficiency of the protein.

5.1. Characterization of folding-defective GALC variants

GALC is co-translationally translocated inside the ER, where it is glycosylated on six N residues with chains of 14 sugars ($Glc_3Man_9GlcNAc_2$) and where it acquires its native structure (Deane et al. 2011). When the protein is correctly folded, it exits the ER and it goes through the Golgi network, where its sugars are modified, becoming more complex. From the Golgi the protein is sent to the lysosomes, where it undergoes its final maturation step, which

is the cleavage in two subunits, one of 50 kDa and one of 30 kDa (Spratley and Deane 2016).

We generated five plasmids for the expression of GALC variants in mammalian cells. An HA tag was placed on the N-terminal of the protein, while a V5 tag was placed at the C-terminal. This was done to follow the formation of the 50 kDa and 30 kDa GALC fragments, due to the successful maturation and delivery to lysosomes. Unfortunately, our system was unsuccessful in the detection of these subunits and we were not able to see the fragments by analysing the TCE or by immunoprecipitating the samples, to concentrate the proteins and allow a better detection. Probably the tags are removed once the protein reach the inside of the lysosomes and undergoes the final maturation step (formation of the fragments), since we were able to detect with WB the ER retained form and the secreted protein using both tags. On the other hand, panels obtained with the confocal microscope showed that the folding-competent variants are successfully delivered to lysosomes. Moreover, by looking at the quantification of loaded lysosomes obtained with LysoQuant, we can confirm also that the delivery is inversely proportional to the degree of severity of the disease (G270D is delivered more than the other folding-defective variants, but less than the WT form).

5.2. Mature GALC is secreted in the extracellular environment

GALC can be delivered to lysosomes by intracellular pathway or via secretion and reuptake from the extracellular environment. This is possible because of M6P receptors located on the cellular membrane, that recognize secreted GALC and allow for its internalization. The enzyme is then delivered to lysosomes via endosomal pathway (Nagano, Yamada et al. 1998).

Since the detection of GALC fragments was unsuccessful, we decided to try another approach to find a proper readout that could assess if the folding and maturation of the protein was successful. The results obtained in the WB analysis showed that GALC can be found in the cellular culture media in

the WT and in the G270D variants, which are the only two folding-competent among the five variants analysed. Moreover, it was observed that the secretion is proportional with the severeness of the disease, being the G270D variant less secreted than the WT (Lee, Kang et al. 2010). This is probably because the exit from the ER depends on the degree of folding efficiency of the enzyme and even if the mutant can fold successfully, it happens in less extent with respect to the WT. EndoH assays also confirms that what we found in the extracellular media is indeed the mature form of GALC, after its passage through the Golgi. By comparing the EndoH assays of the intracellular recovered protein and the extracellular secreted protein, the molecular weight shift observed in the first one (due to the removal of EndoH sensitive sugars) is not detected in the second one, meaning that the protein has indeed passed the ER quality control machinery and has also undergo modifications inside the Golgi, before being secreted.

5.3. Conclusive remarks

We set up a cell-based system that recreates Krabbe disease to assess GALC maturation and intracellular trafficking, using the plasmids that we designed. Since it was very difficult to assess the maturation by looking at the fragments generated inside lysosomes, analysing the extracellular media to detect the secreted protein is indeed the most efficient way to understand if the protein is retained or not in the ER.

This type of experiment could be useful in the event of testing pharmacological chaperones to improve GALC folding properties. These molecules, when administered to patients, should help the targeted enzyme to fold correctly, restoring its enzymatic activity and improving the life of patients. If we see an increase of secretion when transfected cells are treated with a specific chaperone, it could mean that it successfully had a positive impact in promoting the folding of a folding-defective GALC mutant.

The administration of such chaperones could be coupled with an ERT to improve the quality of life and the survivability of KD patients.

6. SUPPLEMENTARY CHAPTER

This side project was focused on the study of the behaviour of three ER-phagy receptors (SEC62, FAM134B, TEX264) under ER stress conditions and autophagy induction. The aim of this study was to understand if there are some stimuli that can selectively increase or decrease ER-phagy processes for a particular receptor, without interfering with the others. This could lead to a better understanding of the cellular response after specific stress conditions, with the activation of particular cellular pathways.

6.1. HaloTag

To perform this kind of study, it was chosen to track the delivery of ER-phagy receptors to lysosomes. This is an indication of an ongoing ER-phagy process, where portions of the ER are sent to lysosomes for degradation (Introduction 1.1.7). The method chosen to perform this tracking was tagging the endogenous ER-phagy receptors SEC62, FAM134B and TEX264 with the HaloTag. This tag is a modified haloalkane dehalogenase designed to covalently bind synthetic ligands. These ligands can be of various nature, such as fluorescent dyes, affinity handles or solid surfaces (Los et al. 2008).
It has been proven that the HaloTag, when delivered to lysosomes in the presence of the fluorescent ligand TMR (2,6-dideoxy-4-S-methyl-4-thio-beta-D-ribo-hexopyranose), generates a protease resistant, fluorescent HaloTag fragment. This fragment is generated from the cleavage of the HaloTag by the acidic and degradative lysosomal activity (Rudinskiy et al. 2022). The amount of HaloTag fragment generated is proportional to the magnitude of delivery of Halo-tagged receptors to lysosomes, being a useful tool to assess ER-phagy activation.

6.2. CRISPR/CAS9 endogenous tagging

MEF cells were subjected to genome editing through CRISPR/CAS9 technology. The HaloTag was inserted at the C-terminal of the chosen

receptor sequence and the successfully modified clones were selected. This procedure was performed modifying a single receptor at the time, obtaining in the end three different MEF cell lines with the HaloTag inserted after the sequence of only one receptor.

6.3. Nutrients starvation

The first step in the study of these cell lines was to observe the formation of the HaloTag fragment in two conditions: steady state, to see the fragment level in absence of stresses (**Fig. 1**, lanes 4-6-8) and with starvation medium (EBSS), which is one of the most prominent triggers of ER-phagy (**Fig. 1**, lanes 5-7-9) (Reggiori and Molinari 2022). We included also control lanes, such as MEF WT, to check if the fragments were truly originated from the HaloTag and one sample treated with BafA1, to check if the fragment was originated thanks to the lysosomal activity.

Cells were seeded in 3,5 cm dishes, 600000 per dish. After 18 hours, cells were incubated with TMR 100 nM, BafA1 100 nM or starvation medium. After 6 hours of incubation with treatments, cells were lysed, subjected to SDS-page in reducing conditions and the resulting gel was analysed to detect the fluorescence emitted from the TMR covalently bonded to the HaloTag.

From the results we can observe the presence of the fragment in the SEC62 and TEX264 samples, at steady state or treated with the starvation medium (**Fig. 1**, lanes 4-5-8-9). We cannot observe the presence of the Halo fragment for the steady state FAM134B receptor (**Fig. 1**, lane 6), while we can observe its presence with starvation medium (**Fig. 1**, lane 7). Meanwhile, we cannot observe any fragments in the control dishes, meaning that the red fluorescent bands that we see on the gel are generated from the endogenous tagging with the HaloTag (**Fig. 1**, lanes 1-2) and that the Halo fragment is generated thanks to lysosomal activity (**Fig. 1**, lane 3). The absence of any visible fragment for the steady state FAM134B can be explained by looking at the intensity of the bands corresponding to the full-length Halo-tagged receptors: the intensity of FAM134B is significantly lower

if compared to SEC62 and TEX264, that could be sign of a lower synthesis of that receptor or wrong extraction conditions for that particular protein in the moment of cellular lysis. It is important to point out the increase of intensity in the fragment bands corresponding to the starvation-treated dishes, with respect to the steady state dishes. This confirms that in presence of ER stresses, such as nutrient starvation, ER-phagy processes regulated by these three receptors increase substantially, increasing the delivery of ER portions to lysosomes and inducing the formation of the Halo fragment.

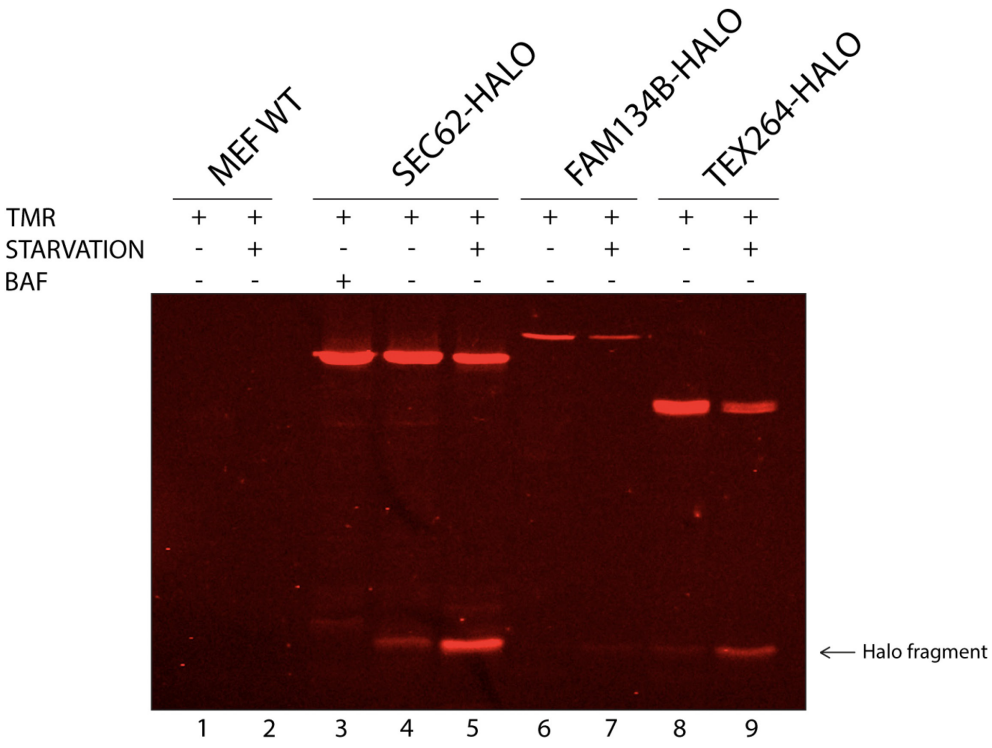

Figure 1: ER-phagy response after nutrient starvation
Endogenous tagged MEF cells of three cell lines (SEC62-HALO, FAM134B-HALO, TEX264-HALO) were cultured for 18 hours in normal cell culture medium and 6 hours with a medium without serum, to mimic nutrient starvation and investigate ER-phagy activity throug the formation of the Halo fragment (lanes 5-7-9). MEF WT were also included as a control, as well as a dish treated with BafA1 (lanes 1-2-3). Cells were also analysed at steady state, to have a reference on basal ER-phagy activity (lanes 4-6-8).

6.4. HaloTag fragment induction with DTT and rapamycin

After assessing the presence of the HaloTag fragment at steady state and nutrient starvation conditions, we decided to subject Halo-tagged cell lines

with other types of stresses that are known to increase ER-phagy activity (Reggiori and Molinari 2022).

Cells were seeded in 3,5 cm dishes, 600000 per dish. For this experiment we focused only on SEC62 and TEX264, since their Halo fragment is easier to detect. After 18 hours, cells were incubated with TMR 100 nM, BafA1 100 nM, DTT 9.6 mM, rapamycin 100 and 200 nM and starvation medium (**Fig. 2**). After 6 hours of incubation with treatments, cells were lysed, subjected to SDS-page in reducing conditions and the resulting gel was analysed.

Rapamycin is a known inhibitor of the mTOR pathway, which is an important protein-kinase that regulates cell proliferation, metabolism and tumor development. Moreover, mTOR activates cellular autophagy when inhibited by rapamycin (Lin et al. 2018) (Reggiori and Molinari 2022). On the other hand, DTT treatment is meant to create a general unbalance in the redox cellular environment and it has been proven to trigger an ER stress response (Xiang et al. 2016).

From our results, we can once again observe an increase in Halo fragment intensity between steady state and nutrient starvation dishes (**Fig. 2**, lanes 1 vs 2, 7 vs 8). These two conditions are important, because they allow us to set two intensities that will be used to evaluate the other treatments: the steady state gives us the basal ER-phagy activity, while nutrient starvation causes a very intense ER-phagy response. As expected, the control lane with BafA1 produced no Halo fragments (**Fig. 2**, lanes 3 and 9).

The dish treated with DTT (**Fig. 2**, lanes 4 and 10) did not show any marked difference between Halo fragment intensities with the steady state dish. An observation on the microscope, prior to the lysis, showed that many cells in the dish were very suffering and a lot of them were floating dead. Probably DTT concentration was too high, causing a general cellular death in the dish, without the possibility to observe an ER-phagy increase.

The treatment with rapamycin, at two different concentrations (**Fig. 2**, lane 5 and 11 100 nM, lane 6 and 12 200 nM), produced a marked increase in

Halo fragment intensity if compared to the steady state dish, but didn't reach the intensity obtained with nutrient starvation. The Halo fragment intensity reached with 200 nM is very similar to the 100 nM dishes, as if rapamycin concentration was already sufficient at 100 nM to reach the maximum ER-phagy trigger.

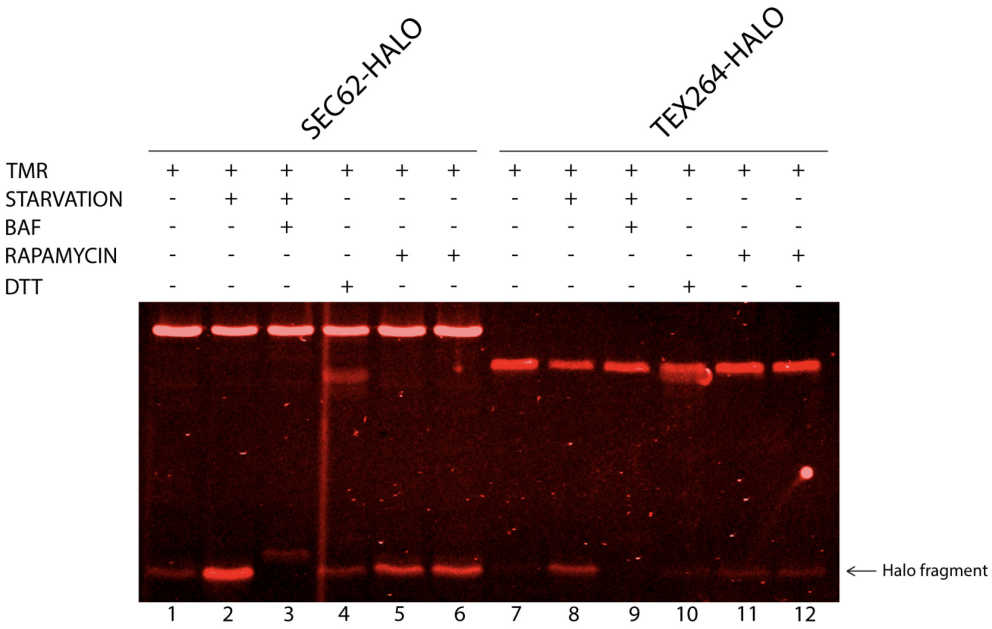

Figure 2: ER-phagy activation after DTT and rapamycin treatments
Endogenous tagged MEF cells of two cell lines (SEC62-HALO, TEX264-HALO) were cultured for 18 hours in normal cell culture medium and 6 hours with nutrient starvation medium (lanes 2-8), BafA1 (lanes 3-9), DTT (lanes 4-10), rapamacyn 100 nM (lanes 5-11) and 200 nM (lanes 6-12) to investigate ER-phagy activity throug the formation of the Halo fragment. Cells were also analysed at steady state, to have a reference on basal ER-phagy activity (lanes 1-7).

6.5. ER-phagy response at different time points under nutrient starvation

Endogenous tagged SEC62-Halo and TEX264-Halo cell lines were subjected to nutrient starvation for different time points, to study if the activation timing of the ER-phagy response could be different among two distinct receptors.

Cells were seeded in 3,5 cm dishes, 600000 per dish. For this experiment as well, we focused only on SEC62 and TEX264. After 18 hours, cells were incubated with TMR 100 nM, BafA1 100 nM, starvation medium (**Fig. 3**). TMR

and BafA1 treatments were made 6 hours prior to lysis. Nutrient starvation time points were 1.5h, 3h, 4.5h and 6h (**Fig. 3**, lanes 2-3-4-5 and 8-9-10-11), where each time represents the duration of the starvation treatment. After the lysis, samples subjected to SDS-page in reducing conditions and the resulting gel was analysed.

By looking at the bands corresponding to the Halo fragment, we noticed that the intensity increased faster in SEC62 than in TEX264. In SEC62 the maximum fluorescence intensity was reached after 4.5 hours (**Fig. 3**, lane 4), being equally intense to the 6 hours band (**Fig. 3**, lane 5). Meanwhile, in TEX264 we observed a progressive increase in fluorescence until 6 hours of treatment (**Fig. 3**, lanes 8 to 11). The increase in intensity of the Halo fragment bands means an increase of ER-phagy receptors delivery to lysosomes, sign of an ongoing ER-phagy process caused by cellular stress.

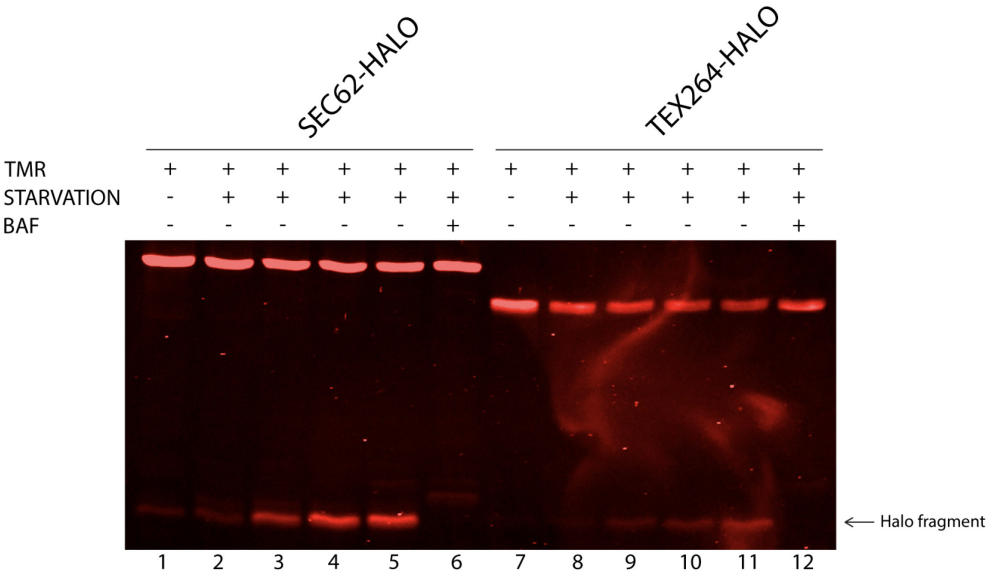

Figure 3: ER-phagy response at different time points under nutrient starvation
Endogenous tagged MEF cells of two cell lines (SEC62-HALO, TEX264-HALO) were cultured for 18 hours in normal cell culture medium and at four time points with nutrient starvation medium (lanes 2 to 5 and 8 to 11) to investigate ER-phagy activity throug the formation of the Halo fragment. Cells were also analysed at steady state, to have a reference on basal ER-phagy activity (lanes 1-7). One dish for each cell line was treated with BafA1 and nutrient starvation medium as a control (lanes 6-12).

6.6. Conclusive remarks

Endogenous tagged ER-phagy receptors, as shown in the experiments carried out in this side project, proved to be a useful tool to follow the activation of the ER-phagy machinery in cells subjected to stressful conditions (nutrient starvation, DTT, rapamycin).

These cell lines can be exploited to study the activation of ER-phagy under specific stress conditions or under the influence of different kind of substances (drugs, toxins, viral infections, etc.), to better understand the impact of various stimuli to cellular homeostasis and organelle remodelling. It has been proven that when ER-phagy receptors, such as SEC62, are overexpressed in some types of tumours, they contribute to drug resistance and low therapy efficacy (Liu et al. 2021), implying that their role could be more impactful than just organelle recycling and remodelling. For this reason, studies on Halo-tagged cell lines could bring light to different approaches when dealing with this kind of diseases, such as combining chemotherapy and other type of drugs, to modulate ER-phagy activity and improve therapy effectiveness.

7. REFERENCES

Aebi, M. (2013). "N-linked protein glycosylation in the ER." Biochim Biophys Acta **1833**(11): 2430-2437.

Ballabio, A. and J. S. Bonifacino (2020). "Lysosomes as dynamic regulators of cell and organismal homeostasis." Nat Rev Mol Cell Biol **21**(2): 101-118.

Braakman, I. and N. J. Bulleid (2011). "Protein folding and modification in the mammalian endoplasmic reticulum." Annu Rev Biochem **80**: 71-99.

Braulke, T. and J. S. Bonifacino (2009). "Sorting of lysosomal proteins." Biochim Biophys Acta **1793**(4): 605-614.

Brockhausen, I., H. Schachter and P. Stanley (2009). O-GalNAc Glycans. Essentials of Glycobiology. nd, A. Varki, R. D. Cummings et al. Cold Spring Harbor (NY).

Brodsky, J. L. and W. R. Skach (2011). "Protein folding and quality control in the endoplasmic reticulum: Recent lessons from yeast and mammalian cell systems." Curr Opin Cell Biol **23**(4): 464-475.

Castonguay, A. C., L. J. Olson and N. M. Dahms (2011). "Mannose 6-phosphate receptor homology (MRH) domain-containing lectins in the secretory pathway." Biochim Biophys Acta **1810**(9): 815-826.

Chen, Y. Q., M. A. Rafi, G. de Gala and D. A. Wenger (1993). "Cloning and expression of cDNA encoding human galactocerebrosidase, the enzyme deficient in globoid cell leukodystrophy." Hum Mol Genet **2**(11): 1841-1845.

Chino, H., Hatta, T., Natsume, T., & Mizushima, N. (2019). "Intrinsically Disordered Protein TEX264 Mediates ER-phagy." Molecular cell, **74**(5), 909–921.e6.

Coutinho, M. F., M. J. Prata and S. Alves (2012). "Mannose-6-phosphate pathway: a review on its role in lysosomal function and dysfunction." Mol Genet Metab **105**(4): 542-550.

Cross, B. C., I. Sinning, J. Luirink and S. High (2009). "Delivering proteins for export from the cytosol." Nat Rev Mol Cell Biol **10**(4): 255-264.

Deane, J. E., S. C. Graham, N. N. Kim, P. E. Stein, R. McNair, M. B. Cachon-Gonzalez, T. M. Cox and R. J. Read (2011). "Insights into Krabbe disease from structures of galactocerebrosidase." Proc Natl Acad Sci U S A **108**(37): 15169-15173.

Fregno, I., Fasana, E., Bergmann, T. J., Raimondi, A., Loi, M., Soldà, T., Galli, C., D'Antuono, R., Morone, D., Danieli, A., Paganetti, P., van Anken, E., & Molinari, M. (2018). "ER-to-lysosome-associated degradation of proteasome-resistant ATZ polymers occurs via receptor-mediated vesicular transport." The EMBO journal, **37**(17), e99259.

Fregno, I., E. Fasana, T. Solda, C. Galli and M. Molinari (2021). "N-glycan processing selects ERAD-resistant misfolded proteins for ER-to-lysosome-associated degradation." EMBO J **40**(15): e107240.

Fregno, I., & Molinari, M. (2019). "Proteasomal and lysosomal clearance of faulty secretory proteins: ER-associated degradation (ERAD) and ER-to-

lysosome-associated degradation (ERLAD) pathways." Critical reviews in biochemistry and molecular biology, **54**(2), 153–163.
Fumagalli, F., Noack, J., Bergmann, T. J., Cebollero, E., Pisoni, G. B., Fasana, E., Fregno, I., Galli, C., Loi, M., Soldà, T., D'Antuono, R., Raimondi, A., Jung, M., Melnyk, A., Schorr, S., Schreiber, A., Simonelli, L., Varani, L., Wilson-Zbinden, C., Zerbe, O., … Molinari, M. (2016). "Translocon component Sec62 acts in endoplasmic reticulum turnover during stress recovery." Nature cell biology, **18**(11), 1173–1184.
Gething, M. J. (1999). "Role and regulation of the ER chaperone BiP." Semin Cell Dev Biol **10**(5): 465-472.
Hebert, D. N. & Molinari, M. (2007) "In and out of the ER: protein folding, quality control, degradation, and related human diseases." Physiol Rev **87**, 1377-1408
Hebert, D. N. & Molinari, M. (2012). "Flagging and docking: dual roles for N-glycans in protein quality control and cellular proteostasis." Trends Biochem Sci **37**, 404-410
Hesketh, G. G., L. Wartosch, L. J. Davis, N. A. Bright and J. P. Luzio (2018). "The Lysosome and Intracellular Signalling." Prog Mol Subcell Biol **57**: 151-180.
Hill, C. H., G. M. Cook, S. J. Spratley, S. Fawke, S. C. Graham and J. E. Deane (2018). "The mechanism of glycosphingolipid degradation revealed by a GALC-SapA complex structure." Nat Commun **9**(1): 151.
Hossain, M. A., T. Otomo, S. Saito, K. Ohno, H. Sakuraba, Y. Hamada, K. Ozono and N. Sakai (2014). "Late-onset Krabbe disease is predominant in Japan and its mutant precursor protein undergoes more effective processing than the infantile-onset form." Gene **534**(2): 144-154.
Ito, Y., & Takeda, Y. (2012). "Analysis of glycoprotein processing in the endoplasmic reticulum using synthetic oligosaccharides." Proceedings of the Japan Academy. Series B, Physical and biological sciences, **88**(2), 31–40.
Kozlov, G., & Gehring, K. (2020). "Calnexin cycle - structural features of the ER chaperone system". The FEBS journal, **287**(20), 4322–4340.
Kriegler, T., Magoulopoulou, A., Amate Marchal, R., & Hessa, T. (2018). "Measuring Endoplasmic Reticulum Signal Sequences Translocation Efficiency Using the Xbp1 Arrest Peptide." Cell chemical biology, **25**(7), 880–890.e3.
Kuribara T, Usui R, Totani K (2021). "Glycan structure-based perspectives on the entry and release of glycoproteins in the calnexin/calreticulin cycle." Carbohydr Research 502:108273.
Lamriben, L., Graham, J. B., Adams, B. M. & Hebert, D. N. (2016). "N-Glycan-based ER Molecular Chaperone and Protein Quality Control System: The Calnexin Binding Cycle." Traffic **17**, 308-326
Lee, W. C., D. Kang, E. Causevic, A. R. Herdt, E. A. Eckman and C. B. Eckman (2010). "Molecular characterization of mutations that cause globoid cell leukodystrophy and pharmacological rescue using small molecule chemical chaperones." J Neurosci **30**(16): 5489-5497.

Lin, X., Han, L., Weng, J., Wang, K., & Chen, T. (2018). "Rapamycin inhibits proliferation and induces autophagy in human neuroblastoma cells." Bioscience reports, **38**(6), BSR20181822.
Liu, X., Su, K., Sun, X., Jiang, Y., Wang, L., Hu, C., Zhang, C., Lu, M., Du, X., & Xing, B. (2021). "Sec62 promotes stemness and chemoresistance of human colorectal cancer through activating Wnt/β-catenin pathway." Journal of experimental & clinical cancer research : CR, **40**(1), 132.
Los, G. V., Encell, L. P., McDougall, M. G., Hartzell, D. D., Karassina, N., Zimprich, C., Wood, M. G., Learish, R., Ohana, R. F., Urh, M., Simpson, D., Mendez, J., Zimmerman, K., Otto, P., Vidugiris, G., Zhu, J., Darzins, A., Klaubert, D. H., Bulleit, R. F., & Wood, K. V. (2008). "HaloTag: a novel protein labeling technology for cell imaging and protein analysis." ACS chemical biology, **3**(6), 373–382.
Martens, S. and H. T. McMahon (2008). "Mechanisms of membrane fusion: disparate players and common principles." Nat Rev Mol Cell Biol **9**(7): 543-556.
Nagano, S., T. Yamada, N. Shinnoh, H. Furuya, T. Taniwaki and J. Kira (1998). "Expression and processing of recombinant human galactosylceramidase." Clin Chim Acta **276**(1): 53-61.
Orsini, J. J., M. L. Escolar, M. P. Wasserstein and M. Caggana (1993). Krabbe Disease. GeneReviews((R)). M. P. Adam, D. B. Everman, G. M. Mirzaa et al. Seattle (WA).
Peotter, J., W. Kasberg, I. Pustova and A. Audhya (2019). "COPII-mediated trafficking at the ER/ERGIC interface." Traffic **20**(7): 491-503.
Pfeffer, S., Dudek, J., Zimmermann, R. & Forster, F. (2016) "Organization of the native ribosome-translocon complex at the mammalian endoplasmic reticulum membrane." Biochim Biophys Acta **1860**, 2122-2129
Platt, F. M., A. d'Azzo, B. L. Davidson, E. F. Neufeld and C. J. Tifft (2018). "Lysosomal storage diseases." Nat Rev Dis Primers **4**(1): 27.
Rafi, M. A., H. Z. Rao, P. Luzi, M. T. Curtis and D. A. Wenger (2012). "Extended normal life after AAVrh10-mediated gene therapy in the mouse model of Krabbe disease." Mol Ther **20**(11): 2031-2042.
Reggio, A., Buonomo, V., Berkane, R., Bhaskara, R. M., Tellechea, M., Peluso, I., Polishchuk, E., Di Lorenzo, G., Cirillo, C., Esposito, M., Hussain, A., Huebner, A. K., Hübner, C. A., Settembre, C., Hummer, G., Grumati, P., & Stolz, A. (2021). "Role of FAM134 paralogues in endoplasmic reticulum remodeling, ER-phagy, and Collagen quality control." EMBO reports, **22**(9), e52289.
Reggiori, F. and M. Molinari (2022). "ER-phagy: mechanisms, regulation, and diseases connected to the lysosomal clearance of the endoplasmic reticulum." Physiol Rev **102**(3): 1393-1448.
Rigante, D., C. Cipolla, U. Basile, F. Gulli and M. C. Savastano (2017). "Overview of immune abnormalities in lysosomal storage disorders." Immunol Lett **188**: 79-85.

Rudinskiy, M., Bergmann, T. J., & Molinari, M. (2022). "Quantitative and time-resolved monitoring of organelle and protein delivery to the lysosome with a tandem fluorescent Halo-GFP reporter." Molecular biology of the cell, **33**(6), ar57.

Sakai, N., K. Inui, N. Fujii, H. Fukushima, J. Nishimoto, I. Yanagihara, Y. Isegawa, A. Iwamatsu and S. Okada (1994). "Krabbe disease: isolation and characterization of a full-length cDNA for human galactocerebrosidase." Biochem Biophys Res Commun **198**(2): 485-491.

Schwarz, D. S. and M. D. Blower (2016). "The endoplasmic reticulum: structure, function and response to cellular signaling." Cell Mol Life Sci **73**(1): 79-94.

Spiegel, R., G. Bach, V. Sury, G. Mengistu, B. Meidan, S. Shalev, Y. Shneor, H. Mandel and M. Zeigler (2005). "A mutation in the saposin A coding region of the prosaposin gene in an infant presenting as Krabbe disease: first report of saposin A deficiency in humans." Mol Genet Metab **84**(2): 160-166.

Spratley, S. J. and J. E. Deane (2016). "New therapeutic approaches for Krabbe disease: The potential of pharmacological chaperones." J Neurosci Res **94**(11): 1203-1219.

Stanley, P. (2011). "Golgi glycosylation." Cold Spring Harb Perspect Biol **3**(4).

Stanley, P., H. Schachter and N. Taniguchi (2009). N-Glycans. Essentials of Glycobiology. nd, A. Varki, R. D. Cummings et al. Cold Spring Harbor (NY).

Wang, J., Lee, J., Liem, D., & Ping, P. (2017). "HSPA5 Gene encoding Hsp70 chaperone BiP in the endoplasmic reticulum". Gene, 618, 14–23.

Wenger, D. A., M. A. Rafi and P. Luzi (1997). "Molecular genetics of Krabbe disease (globoid cell leukodystrophy): diagnostic and clinical implications." Hum Mutat **10**(4): 268-279.

Xiang, X. Y., Yang, X. C., Su, J., Kang, J. S., Wu, Y., Xue, Y. N., Dong, Y. T., & Sun, L. K. (2016). "Inhibition of autophagic flux by ROS promotes apoptosis during DTT-induced ER/oxidative stress in HeLa cells." Oncology reports, **35**(6), 3471–3479.

8. ACKNOWLEDGEMENTS

I'm extremely grateful to Maurizio Molinari, which welcomed me in his laboratory to perform my master thesis work, teaching me how to reason as a researcher and to carry out experiments.

Special thanks to my supervisor Ilaria for being always helpful and patient in oversighting my experiments and for helping me with the writing of my thesis.

Many thanks to Dorianna Sandonà, for introducing me to the IRB and for being always supportive in her role as a supervisor.

I want to thank the other members of the laboratory for all the advice and the support they gave me. You have been amazing lab mates, I really enjoyed my time in the IRB. Thank you, Elisa, Tatiana, Carmela, Marika, Misha and Diego!

Thanks to all the amazing people that I met, especially my flatmates Leonardo, Rebecca, Gaia and Maria Rosaria. I couldn't have done it without you.

Thanks to all my friends that supported me from home and who have always been there in times of need.

Finally, I could not have undertaken this journey without my family, who were always ready to support me in the important moments of my life, such as this journey abroad.